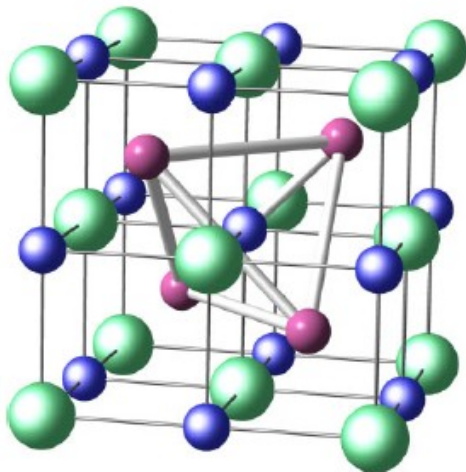


# Stopy Heuslera

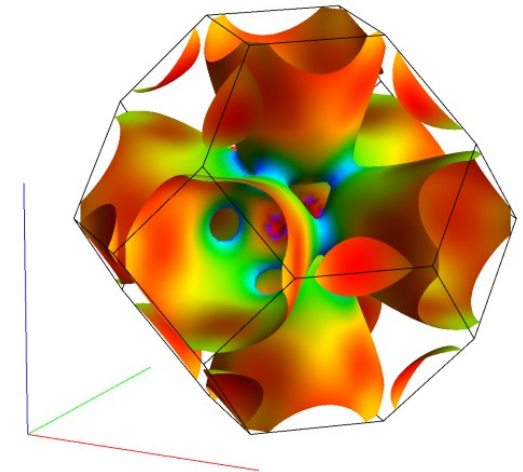
laboratorium własności fizycznych “na życzenie”

Janusz TOBOLA

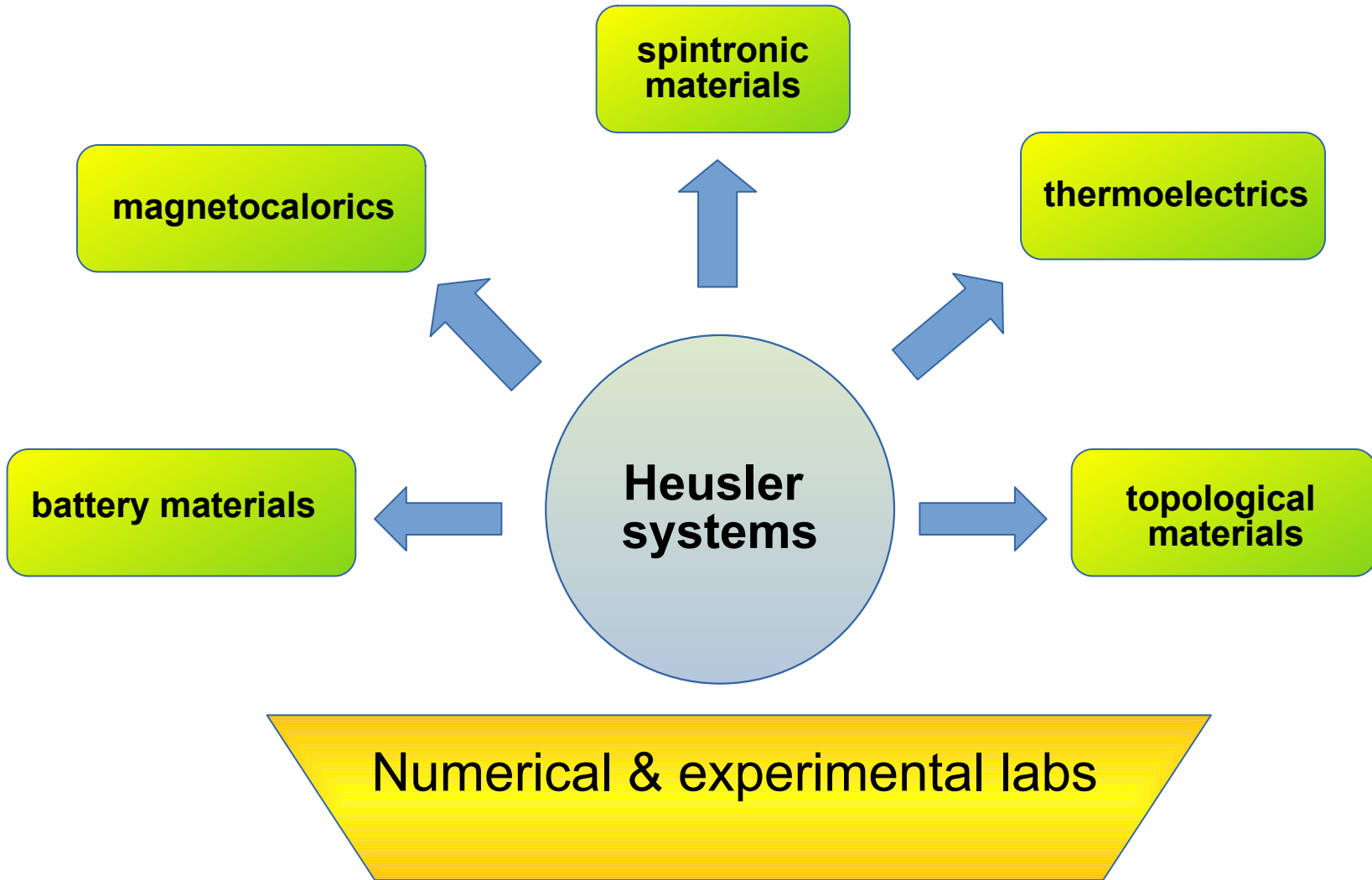
*Katedra Fizyki Materii Skondensowanej  
WFIS AGH*



$$G = G_0 + G_0VG$$



# PLAN



# Discovery of Heusler phases

**1903 – Friedrich Heusler** (mining engineer and chemist) accidentally discovers  $\text{Cu}_2\text{MnAl}$  as a new ferromagnetic compound from “non-ferromagnetic” elements, when mixing Mn with Zn, Cu, As, Sb, Bi and B, but good ferromagnetic properties was obtained when adding Al.

Verhandlungen  
der  
**Deutschen Physikalischen Gesellschaft**

Im Auftrage der Gesellschaft herausgegeben  
von  
**Karl Scheel**

5. Jahrg. 30. Juni 1903. Nr. 12.

**Sitzung vom 12. Juni 1903.**

Vorsitzender: Herr M. PLANCK.

Vor Eintritt in die Tagesordnung verliest Hr. H. Starke auf Wunsch des Hrn. Fr. Heusler eine von diesem durch Vermittelung des Hrn. F. Bicharz am 18. Juni 1901 bei der Gesellschaft niedergelegte Notiz:

Über magnetische Manganlegierungen  
und macht weiter Mitteilung über zwei im Zusammenhang hiermit stehende Arbeiten von Hrn. Fr. Heusler, W. Starck und E. Haupt:

Magnetisch-chemische Studien:

I. Über die Synthese ferromagnetischer Manganlegierungen; von Hrn. FR. HEUSLER  
und

II. Über die magnetischen Eigenschaften von eisenfreien Manganlegierungen; von Hrn. W. STARCK und E. HAUPT.

Alle drei Mitteilungen gelangen weiter unten zum Abdruck.

UNIVERSITY OF ILLINOIS

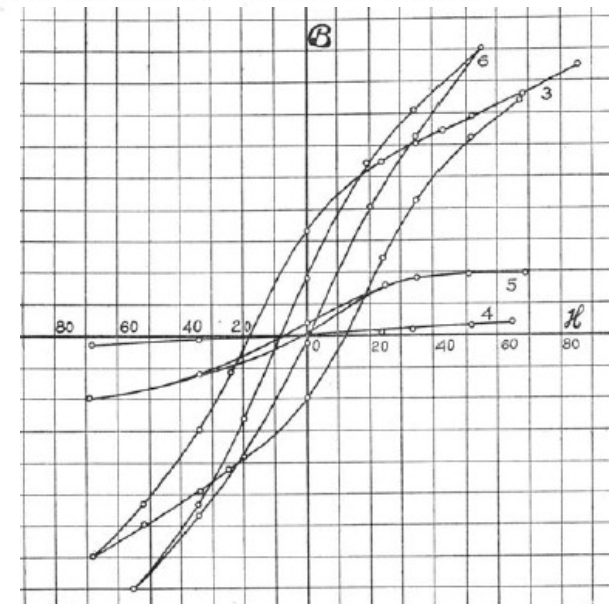
ENGINEERING EXPERIMENT STATION

BULLETIN No. 47

DECEMBER 1910

MAGNETIC PROPERTIES OF HEUSLER ALLOYS

BY EDWARD B. STEPHENSON, FORMERLY ASSISTANT IN PHYSICS



$T_C = 630 \text{ K}$  (high)

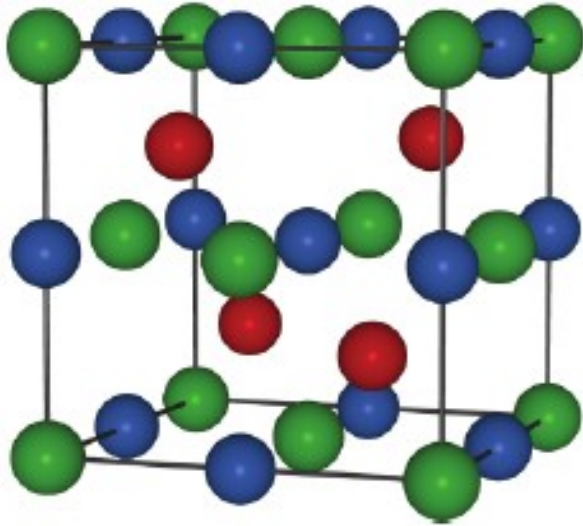
$M = 3.7 \mu_B$

attributed to Mn atoms

RT sat. magnetization strongly depends on heat treatment  
6.1 kGs for Ni < 8kGs < 23 kGs for Fe

# Crystal structure of Heusler phases

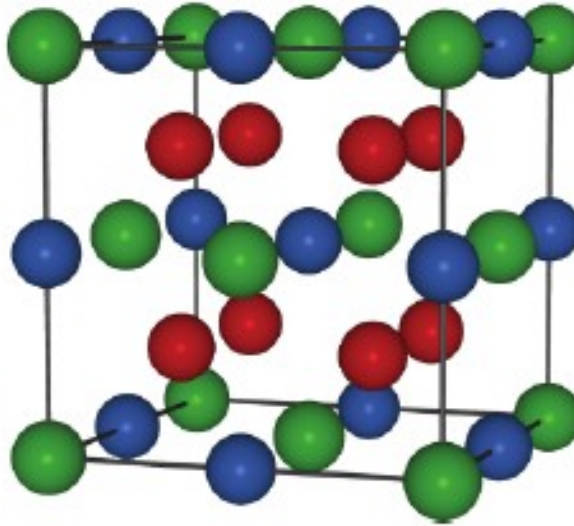
**1934** – A.J. Bradley & J.W. Rogers and independently O. Heusler (son of FH) describe **Cu<sub>2</sub>MnAl** as fully ordered crystal structure of L2<sub>1</sub> type



No. 216, F-43m, C1<sub>b</sub>

**XYZ**

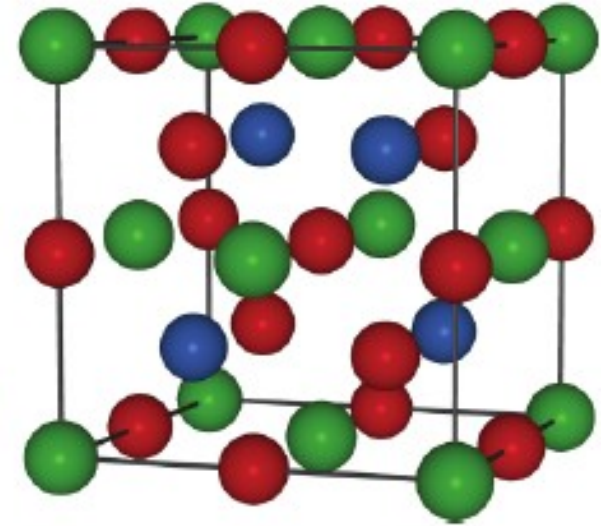
Half-Heusler structure  
LiMgAs(Nowotny) & CuMgAs(Juza)



No. 225, Fm3m, L2<sub>1</sub>

**X<sub>2</sub>YZ**

Full-Heusler structure



No. 225, X<sub>A</sub>

**XYXZ or XYUZ**

Inverse Heusler structure

L Wollmann, A K Nayak, S. S. P. Parkin, C Felser, Heusler 4.0: Tunable Materials (2017)

Heusler O. 1934. Kristallstruktur und Ferromagnetismus der Mangan-Aluminium- Kupferlegierungen. Adv. Phys. 411, 155- 201

Bradley AJ, Rogers JW. 1934. The crystal structure of the Heusler alloys. Proc. Roy. Soc. (London) A 144, 340- 359

# Heusler phases $X_2YZ$ , $XYZ$

## structure $DO_3$

***Fm3m*** (type  $Fe_3Al$ )

$X : (0,0,0), (1/2,1/2,1/2)$

$X : (3/4,3/4,3/4)$

$Z : (1/4,1/4,1/4)$

## Normal Heusler $L2_1$

***Fm3m*** (type  $Cu_2MnAl$ )

$X : (0,0,0), (1/2,1/2,1/2)$

$Y : (3/4,3/4,3/4)$

$Z : (1/4,1/4,1/4)$

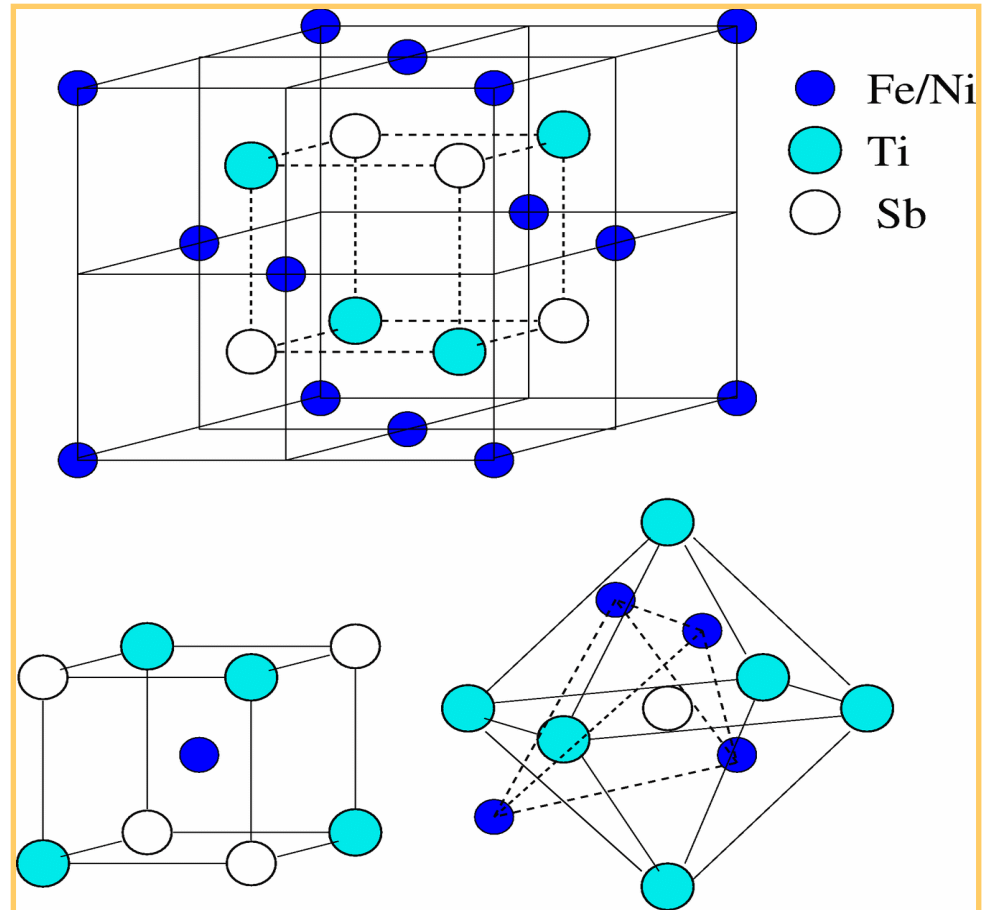
## Half-Heusler $C1_b$

***F-43m*** (type  $AgMgAs$ )

$X : (0,0,0) \quad 4a$

$Y : (3/4,3/4,3/4) \quad 4d$

$Z : (1/4,1/4,1/4) \quad 4c$



**Crystal stability**  
**orbitals  $sp^3, d$**

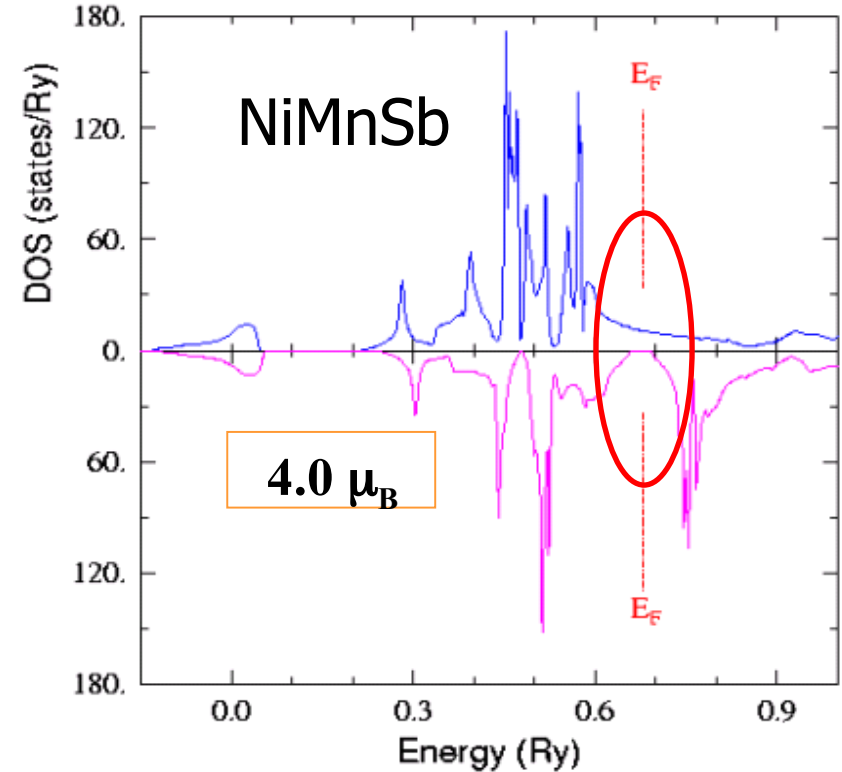
# Half-Heusler phases

## Wide variety of physical behaviours

- \* metals, semiconductors, semimetals
- \* strong and weak FM, AFM (high  $T_C / T_N$ )
- \* Pauli paramagnets, Curie-Weiss PM
- \* half-metallic ferromagnets (HFM)
- \* strong thermoelectrics

## Half-metallic ferromagnetism

- \* lack of FS for one spin direction
- \* integer magnetic moment value
- \* anomalous  $\rho(T)$  dependence
- \* giant magneto-optic Kerr effect
- \* predictions of HM-AF (1993)
- \* HFM :  $\text{CrO}_2$ ,  $(\text{La-Sr})\text{MnO}_3$ , spinels
- \* spintronic materials



ME 50, NUMBER 25      PHYSICAL REVIEW LETTERS      20 JUNE 1983

---

**New Class of Materials: Half-Metallic Ferromagnets**  
 R. A. de Groot and F. M. Mueller  
*Research Institute for Materials, Faculty of Science, Toernooiveld, 6525 ED Nijmegen, The Netherlands*

and  
 P. G. van Engen and K. H. J. Buschow  
*Philips Research Laboratories, 5600 JA Eindhoven, The Netherlands*

(Received 21 March 1983)

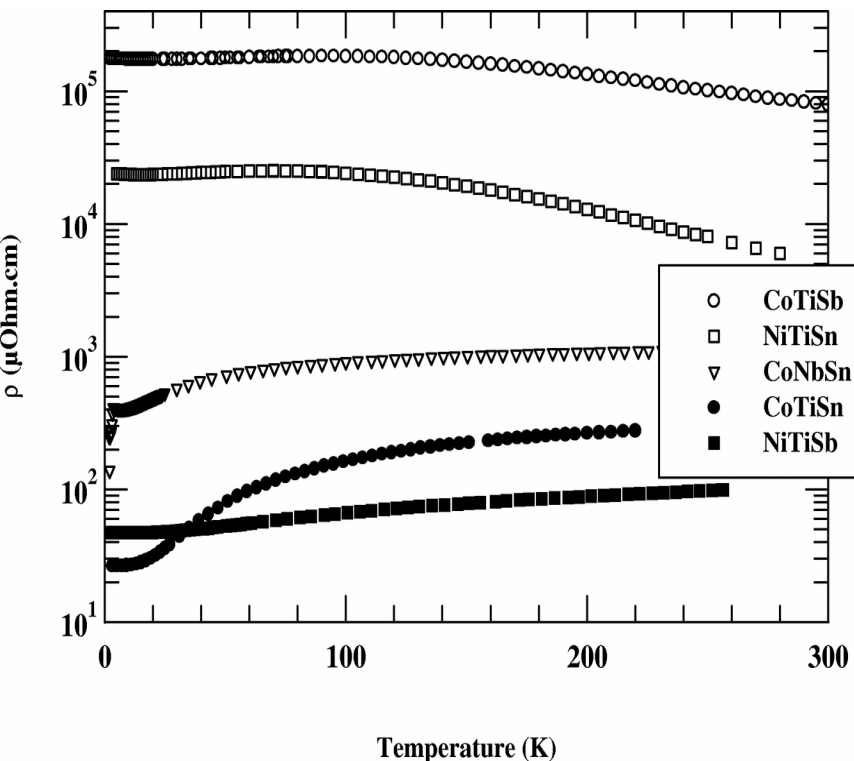
The band structure of Mn-based Heusler alloys of the  $\text{Cl}_b$  crystal structure (MgAgAs type) has been calculated with the augmented-spherical-wave method. Some of these magnetic compounds show unusual electronic properties. The majority-spin electrons are metallic, whereas the minority-spin electrons are semiconducting.

# Electron phase diagram of half-Heusler systems

*JT et al., JMMM (1996), J. Phys. CM (1998), JALCOM (2000)*

~ 650 citations

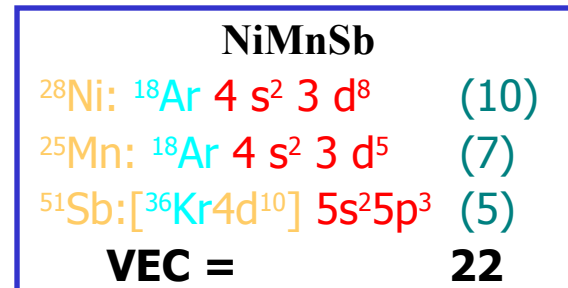
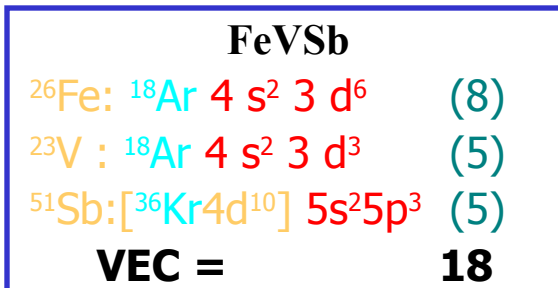
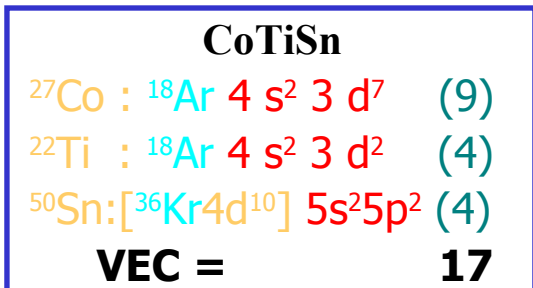
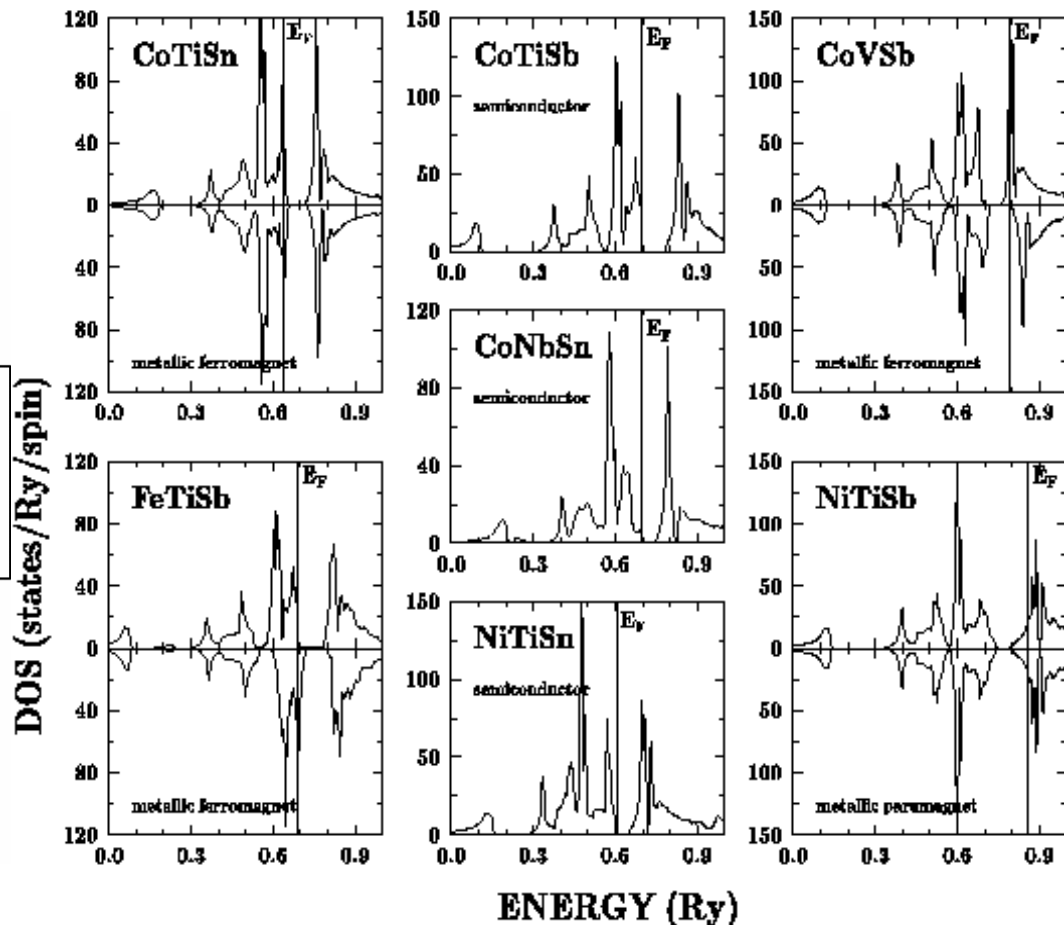
## Electrical resistivity



17 valence electrons

18 valence electrons

19 valence electrons



# Variety of physical properties of HH

EVIER

Journal of Alloys and Compounds 262-263 (1997) 101-107

## Properties on request in semi-Heusler phases

J. Pierre<sup>a,\*</sup>, R.V. Skolozdra<sup>b</sup>, J. Tobola<sup>c</sup>, S. Kaprzyk<sup>c</sup>, C. Hordequin<sup>a</sup>, M.A. Kouacou<sup>a</sup>,  
I. Karla<sup>a</sup>, R. Currat<sup>d</sup>, E. Lelièvre-Berna<sup>d</sup>

<sup>a</sup>Laboratoire L.NEEL, CNRS, 166X, 38042 Grenoble, France

<sup>b</sup>Dept of Inorganic Chemistry, I.FRANKO University, 290005 Lviv, Ukraine

<sup>c</sup>Faculty of Physics and Nuclear Techniques, Academy of Mining and Metallurgy, 30-073 Krakow, Poland

<sup>d</sup>Institut Laue Langevin, 156X, 38042 Grenoble, France

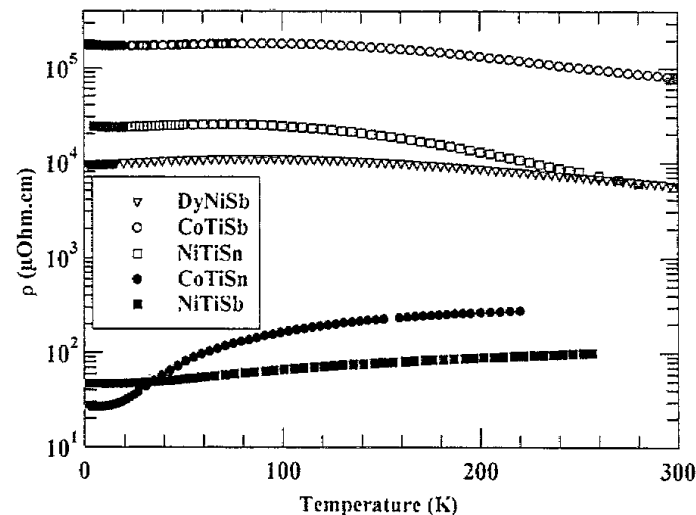
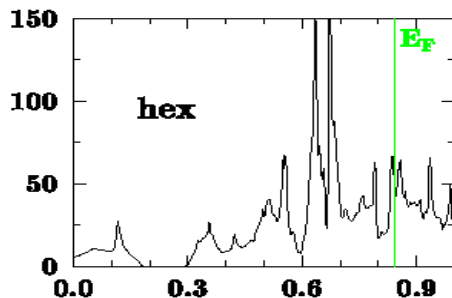
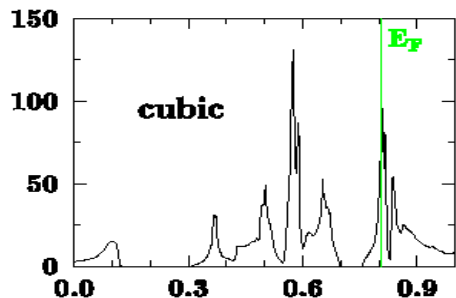


Fig. 1. Resistivity for some semi-Heusler phases.

Lattice parameter (300 K), Curie, Néel and Curie-Weiss temperatures, ordered and paramagnetic moments for some semi-Heusler phases

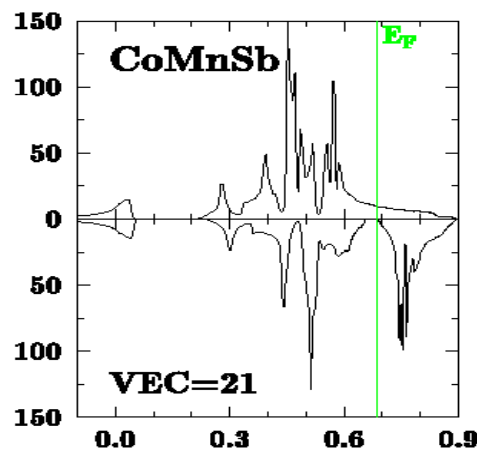
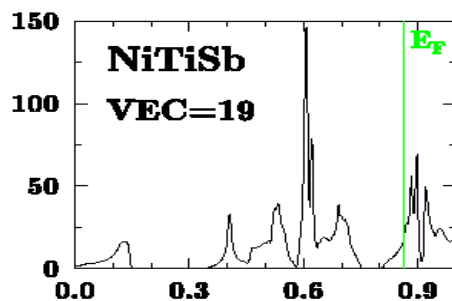
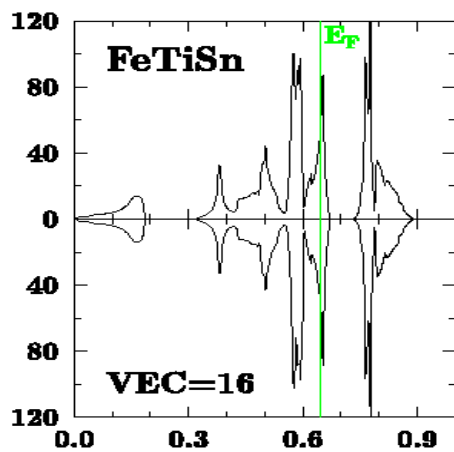
Phase	$a$ (Å)	$T_c, T_N$ (K)	$M(0)$ ( $\mu_B$ )	$\theta_p$ (K)	$M_{\text{eff}}$ ( $\mu_B$ )	$10^4 \chi$ (emu mol <sup>-1</sup> )
CoTiSn	5.997	$T_c = 135$	0.357	158	1.35	—
CoTiSb	5.884	—	—	—	—	1.7
CoNbSn	5.947	—	—	—	—	0.53
NiTiSn	5.947	—	—	—	—	1.3
CoVSb	5.791	$T_c = 11-58$	0.04-0.18	15-75	0.9-1.26	—
NiTiSb	5.872	—	—	—	—	1.4
NiTbSb	6.310	$T_N = 5.5$	5.6	-17	9.7	—
NiDySb	6.305	3.5	—	-8	10.9	—
NiHoSb	6.286	2.5	—	-7.5	10.7	—
NiMnSb	5.930	$T_c = 730$	4.02	~ 900	4.5-2.9	—





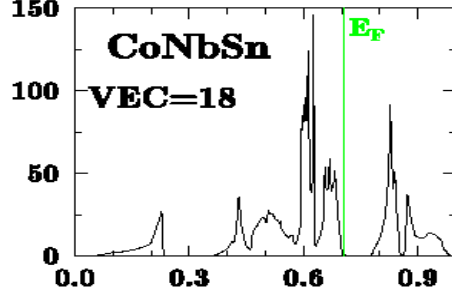
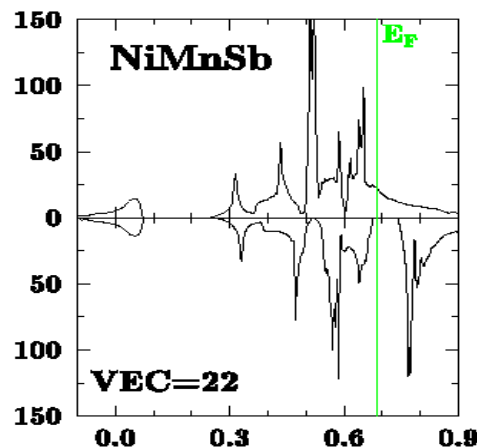
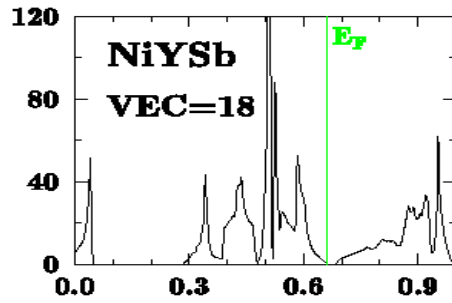
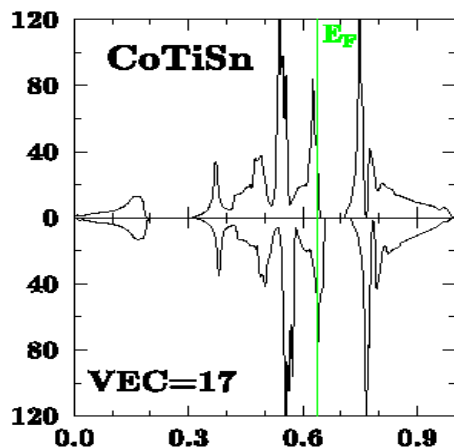
Properties  
"on request"

**ELECTRONIC PHASE DIAGRAM OF HALF-HEUSLER SYSTEMS**



Phase transitions

- FM-PM
- FM-HMF
- FM-SC
- PM-SC
- PM-SC-PM
- FM-SC-PM



# Theory of Brillouin Zones and Symmetry Properties of Wave Functions in Crystals

L. P. BOUCKAERT,\* R. SMOLUCHOWSKI AND E. WIGNER, *The Institute for Advanced Study Princeton University, Princeton, New Jersey and the University of Wisconsin*

TABLE I. Characters of small representations of  $\Gamma$ ,  $R$ ,  $H$ .

$\Gamma, R, H$	$E$	$3C_4^2$	$6C_4$	$6C_2$	$8C_3$	$J$	$3JC_4^2$	$6JC_4$	$6JC_2$	$8JC_3$
$\Gamma_1$	1	1	1	1	1	1	1	1	1	1
$\Gamma_2$	1	1	-1	-1	1	1	1	-1	-1	1
$\Gamma_{12}$	2	2	0	0	-1	2	2	0	0	-1
$\Gamma_{15}'$	3	-1	1	-1	0	3	-1	1	-1	0
$\Gamma_{25}'$	3	-1	-1	1	0	3	-1	-1	1	0
$\Gamma_1'$	1	1	1	1	1	-1	-1	-1	-1	-1
$\Gamma_2'$	1	1	-1	-1	1	-1	-1	1	1	-1
$\Gamma_{12}'$	2	2	0	0	-1	-2	-2	0	0	1
$\Gamma_{15}$	3	-1	1	-1	0	-3	1	-1	1	0
$\Gamma_{25}$	3	-1	-1	1	0	-3	1	1	-1	0

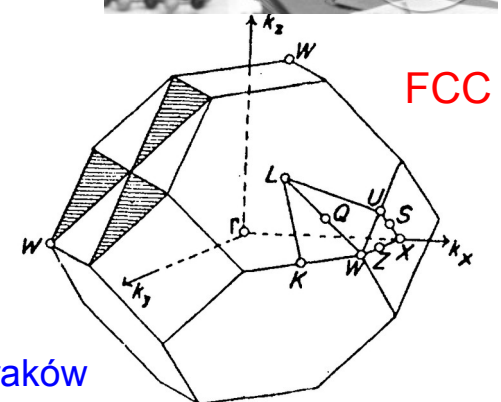
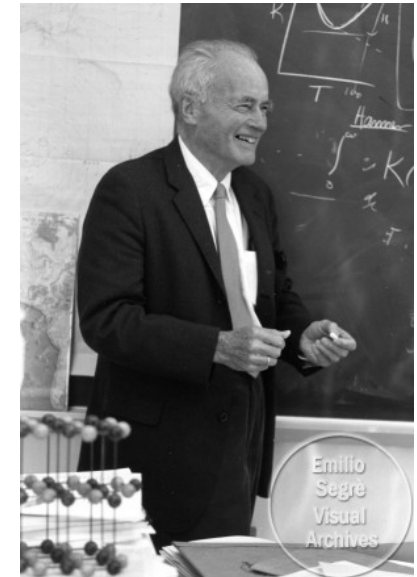
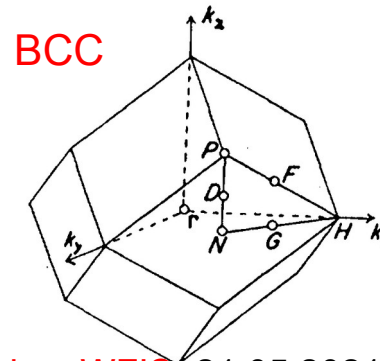
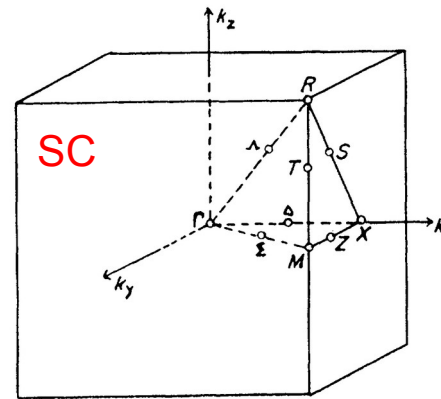
TABLE XIV. Characters of small representations of  $W$ .

$W$	$E$	$C_4^2$	$2C_2$	$2JC_4$	$2JC_4^2$
$W_1$	1	1	1	1	1
$W_1'$	1	1	1	-1	-1
$W_2$	1	1	-1	1	-1
$W_2'$	1	1	-1	-1	1
$W_3$	2	-2	0	0	0

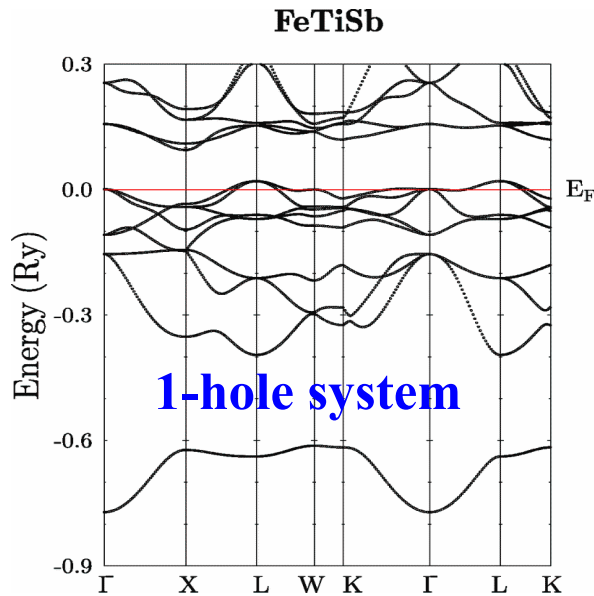
TABLE XV. Characters of small representations of  $L$ .

$L$	$E$	$2C_3$	$3C_2$	$J$	$2JC_3$	$3JC_2$
$L_1$	1	1	1	1	1	1
$L_2$	1	1	-1	1	1	-1
$L_3$	2	-1	0	2	-1	0
$L_1'$	1	1	1	-1	-1	-1
$L_2'$	1	1	-1	-1	-1	1
$L_3'$	2	-1	0	-2	1	0

notation BSW for energy dispersion bands in BZ derived from Bloch states in crystals with basic structures SC, BCC & FCC (symmetry theory and characters of representations)

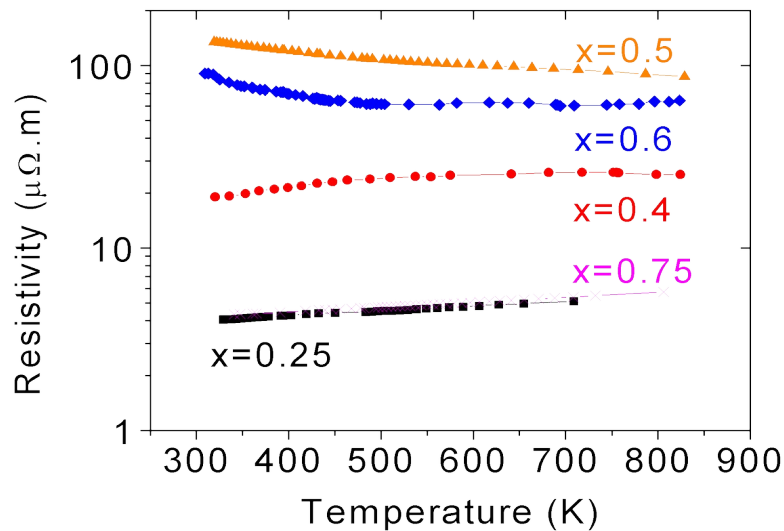
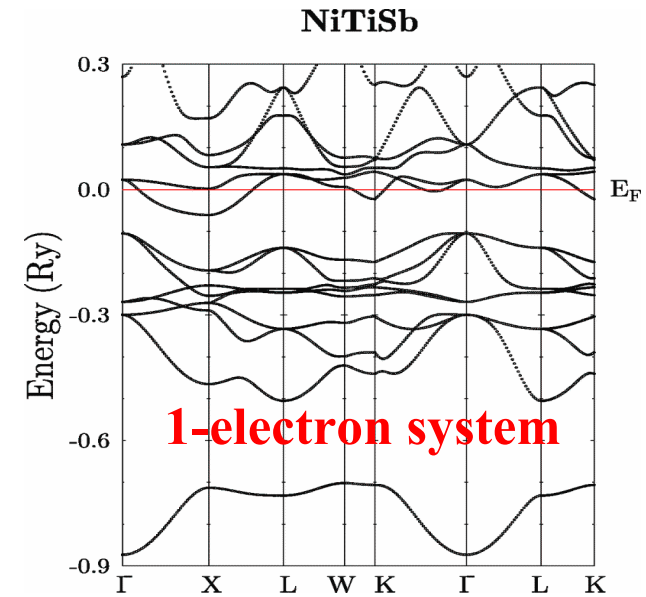


# Metal–semiconductor-metal crossovers

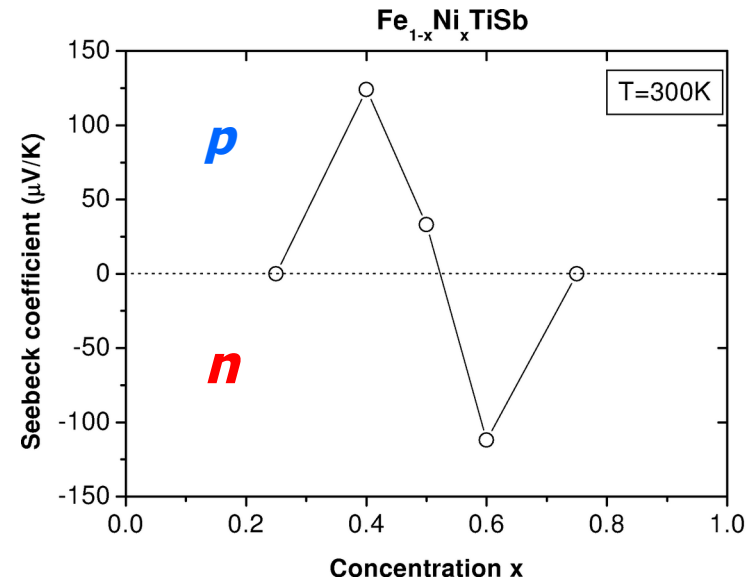


FeTiSb (VEC=17)  
 Curie-Weiss PM ( $\sim 0.9\mu_B$ )  
 NiTiSb (VEC=19)  
 Pauli PM

*JT et al., PRB 64, 155103 (2001)*

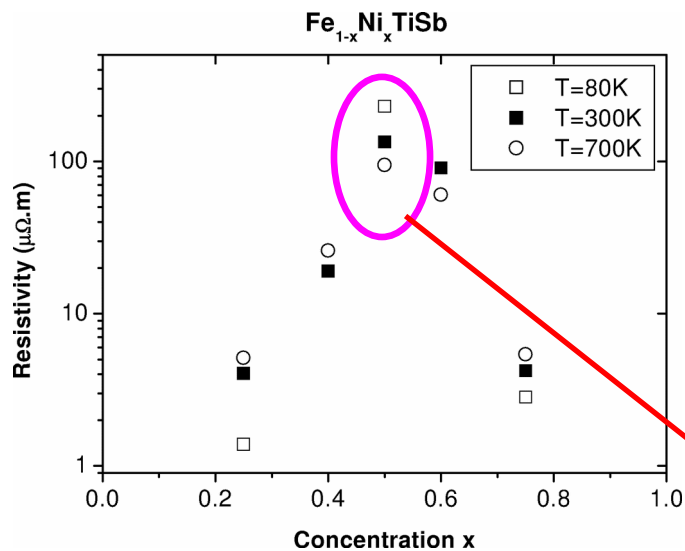


**Resistivity (experiment)**

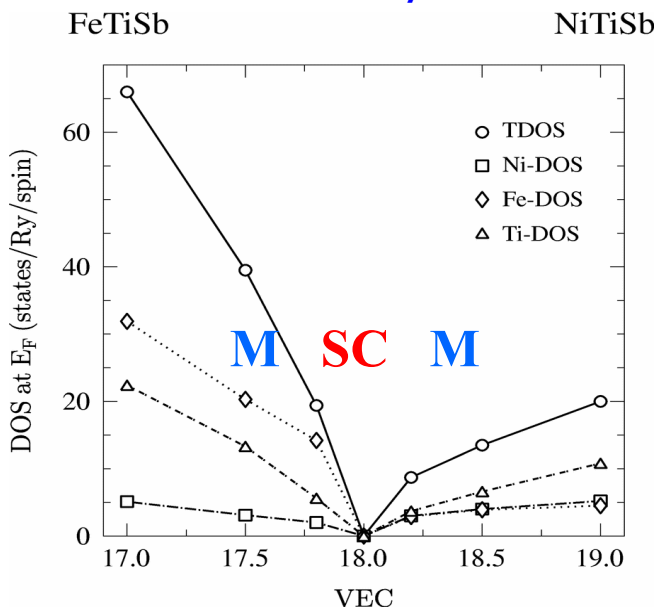


**Thermopower (experiment)**

# Semiconductor from alloyed metals

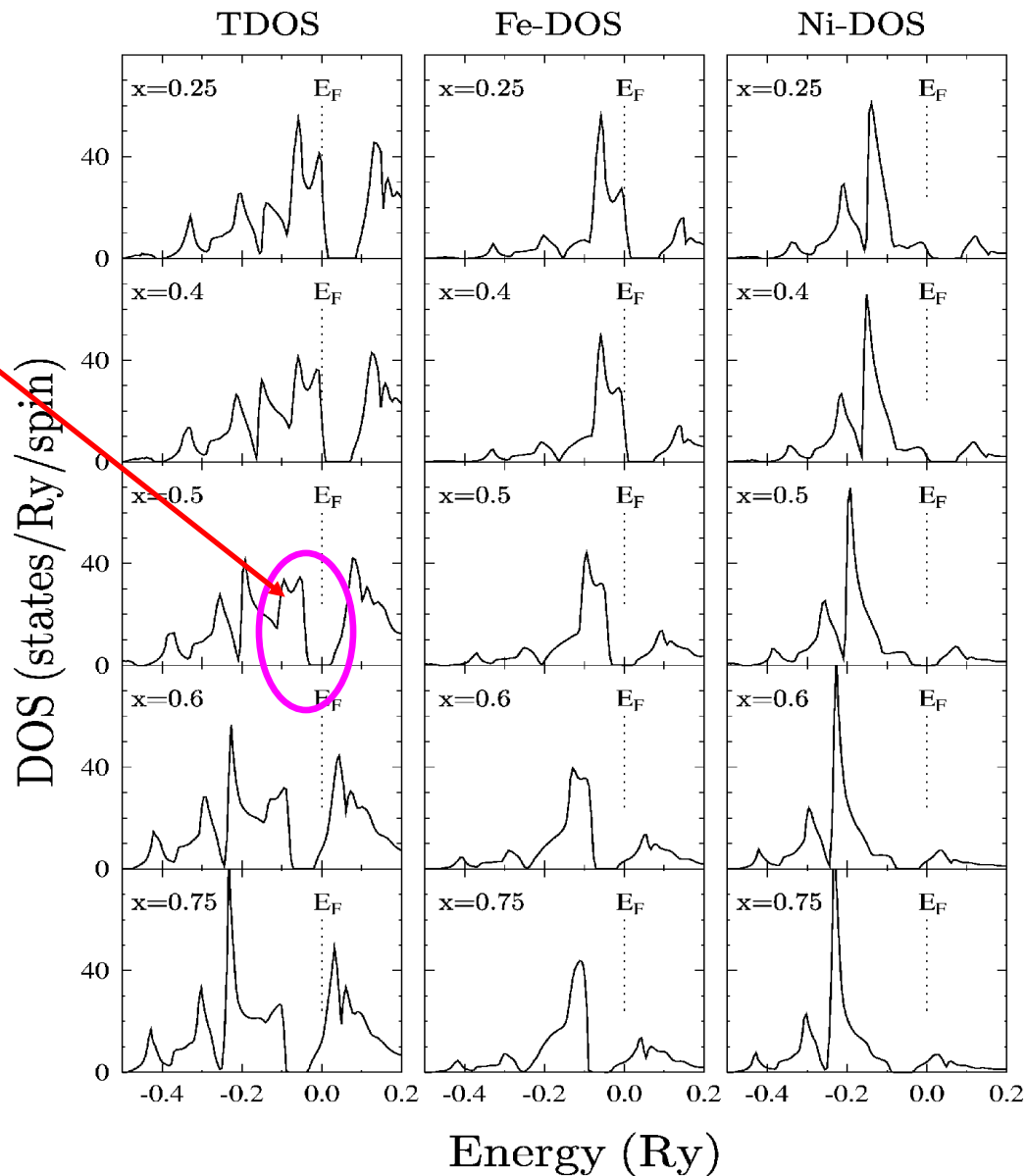


Resistivity

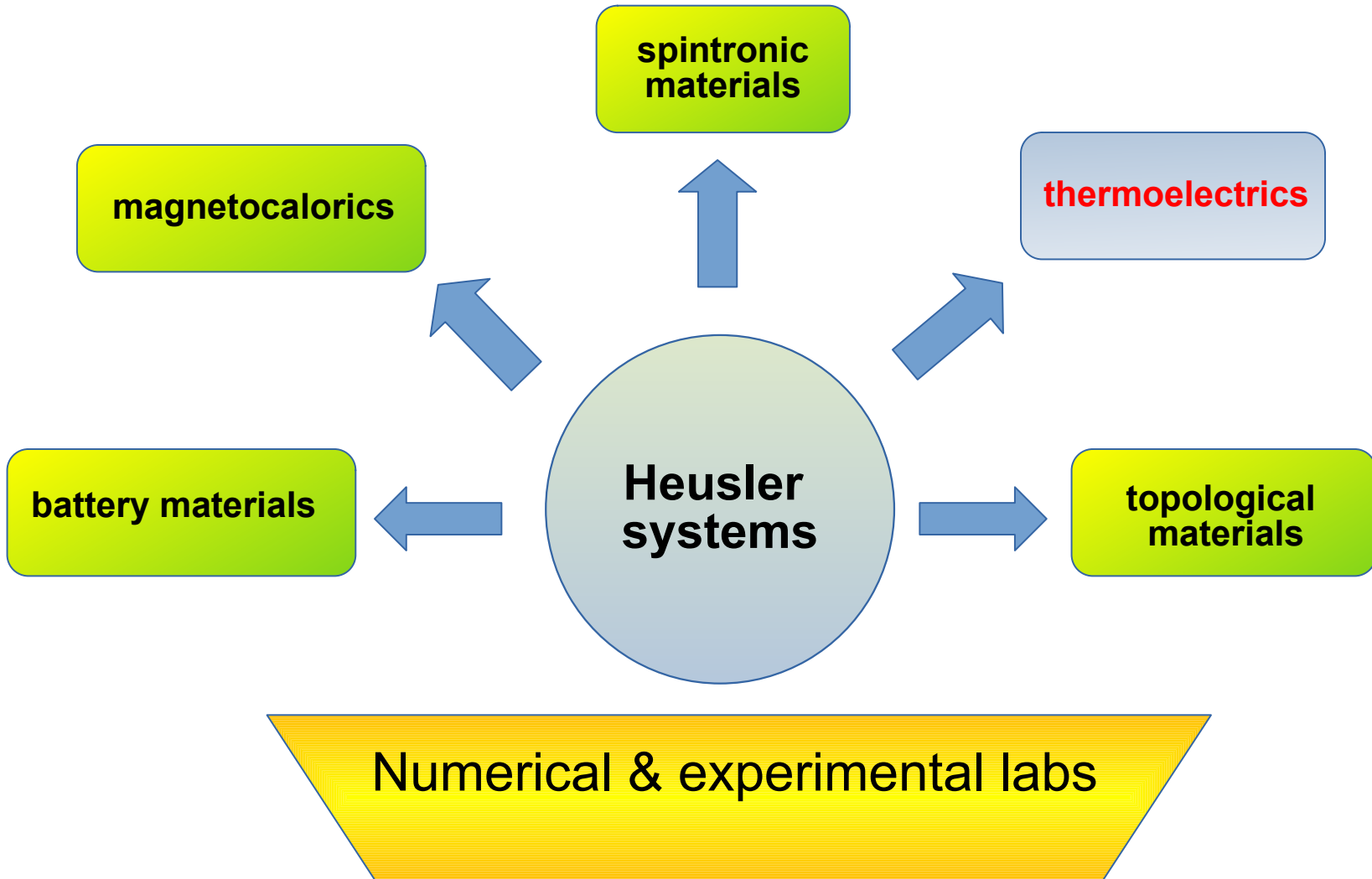


Density of states at  $E_F$

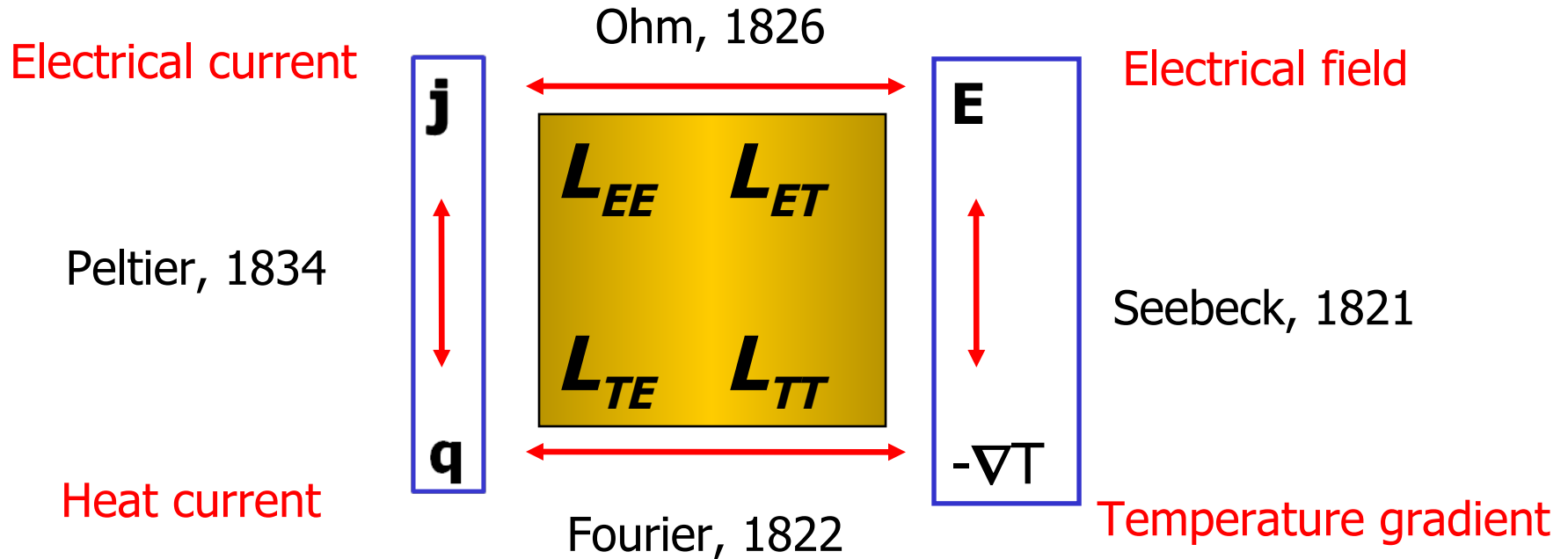
## $\text{Fe}_{1-x}\text{Ni}_x\text{TiSb}$



# PLAN



# Thermoelectric „tetragon”



$$S T = \Pi \quad (\text{Thomson-Kelvin-Onsager}) \quad L_{ET} = L_{TE} / T$$

$$\kappa / \sigma \approx L_0 T \quad (\text{Wiedemann-Franz, } L_0 \text{ Lorentz number}) \quad \kappa \approx -L_{TT}$$

Volta (1800), Ampere (1820), Faraday (1831), Gauss (1832), ...

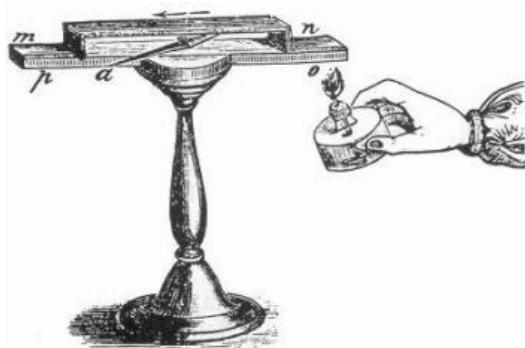
# Thermoelectric properties

## search for optimum

Improvement of figure of merit



Geometry of the devices



Physical properties of the system



*Carnot limit*

COOLING ELEMENTS

$$COP = (T_H - T_C)(\gamma - 1)(T_C + \gamma T_H)^{-1}$$

POWER GENERATORS

$$\eta = (\gamma T_C - T_H)[(T_H - T_C + (\gamma + 1))]^{-1}$$

$$\gamma = (1 + ZT)^{1/2}$$



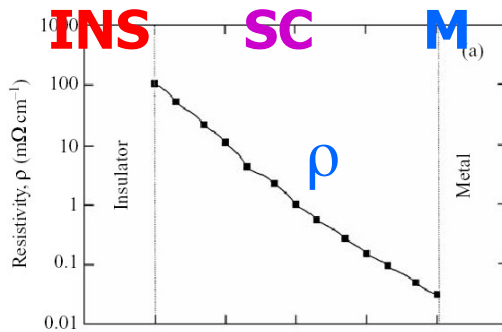
A.F. Ioffe

$$ZT = \frac{S^2 \sigma}{\kappa} T = \underbrace{\frac{S^2}{L}}_{\text{calculated}} \frac{1}{1 + \frac{\kappa_L}{\kappa_e}}$$

Lorentz factor

Thermal conductivity  
(phonons / electrons)

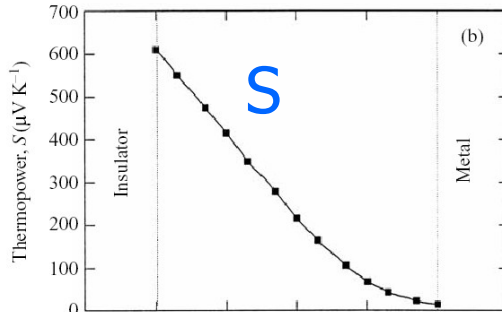
Resitivity



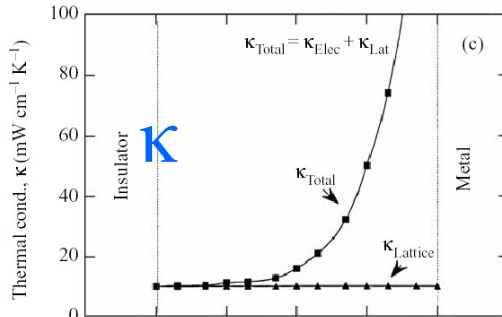
# Thermoelectric properties

$$ZT = \frac{S^2 \sigma}{K} T$$

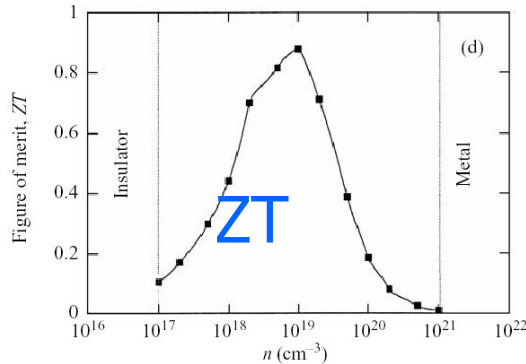
Thermopower



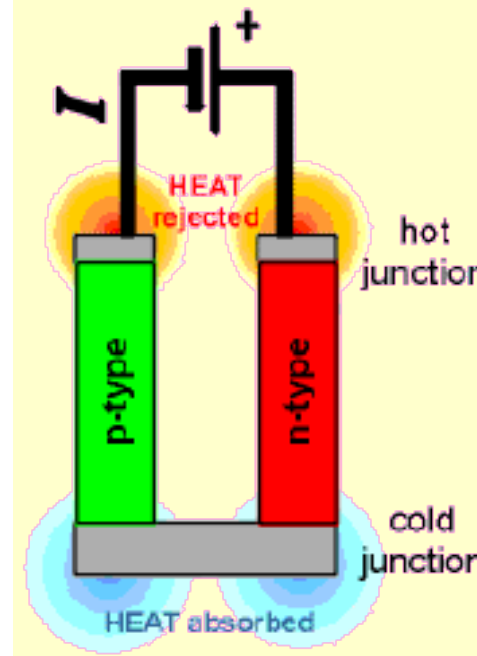
Thermal conductivity



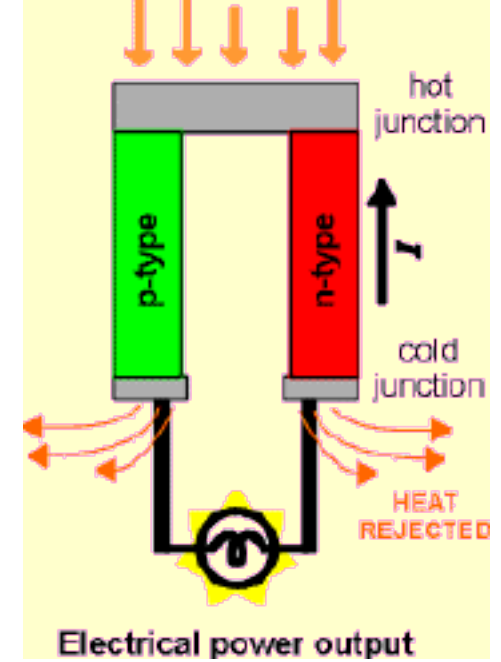
ZT  
Figure of merit



Electrical power input



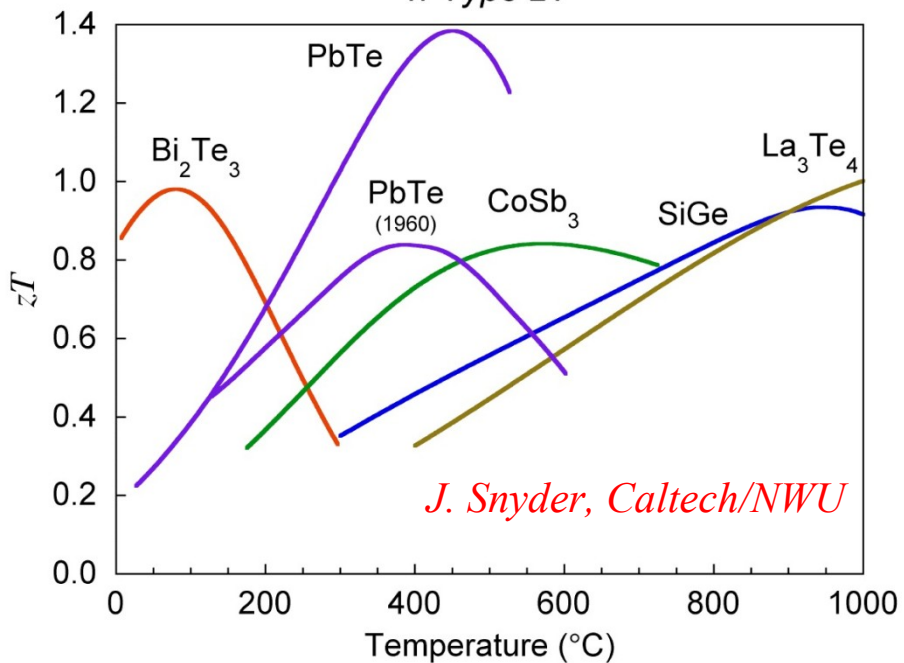
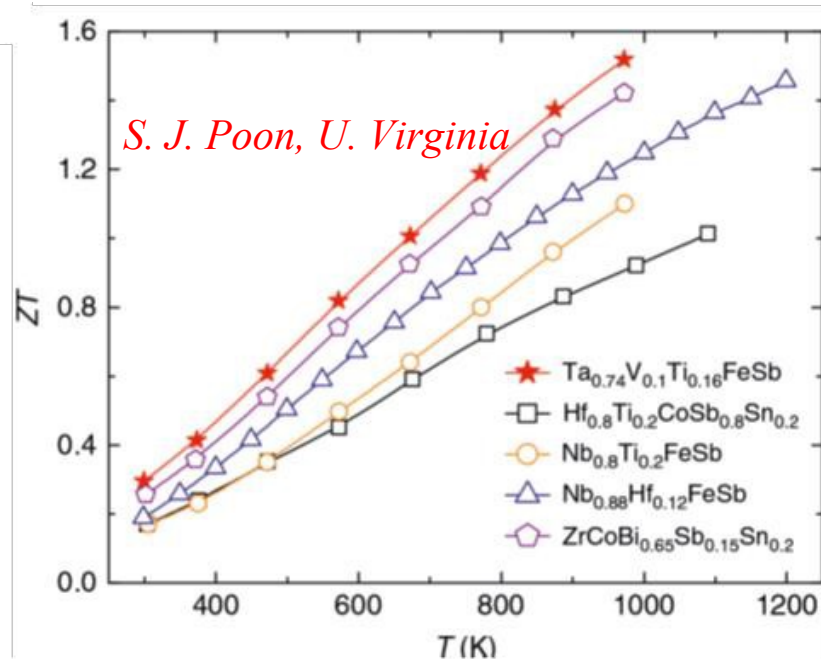
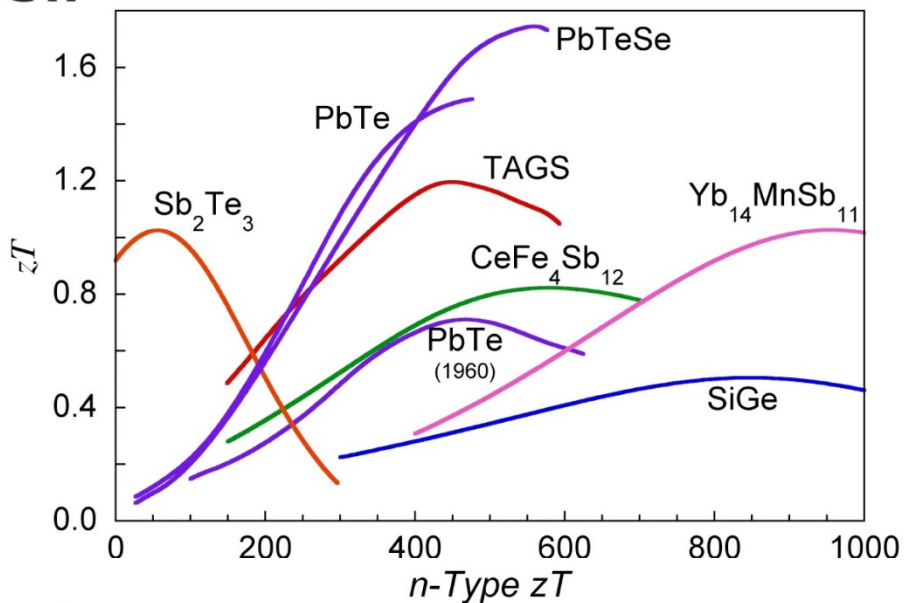
HEAT input



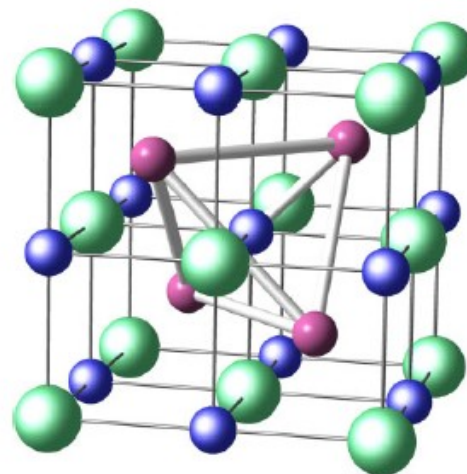


# Thermoelectric materials

*p-Type zT*



## Half-Heusler phases

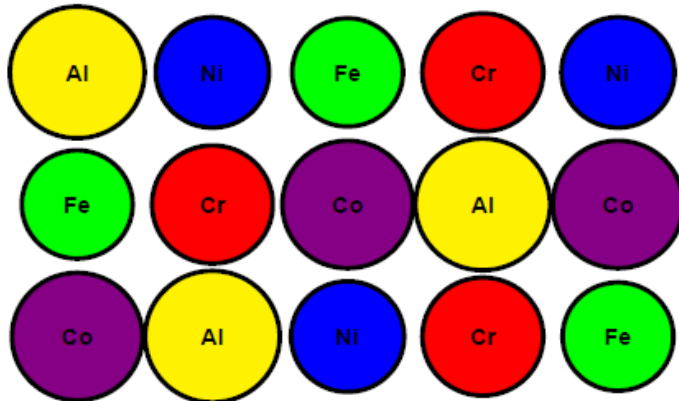


# KKR-CPA method

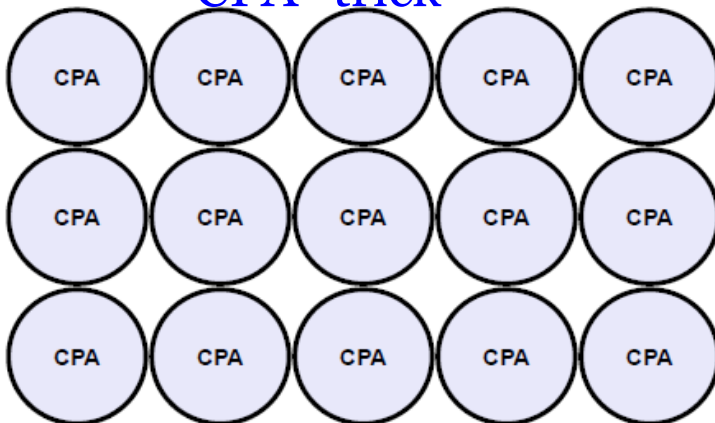


S. Kaprzyk

Disordered alloys: ~~periodic~~ - Coherent Potential Approximation (CPA):



CPA “trick”



$$T_{k'\sigma'L',k\sigma L}^{CP} = \frac{1}{N} \sum_{\mathbf{k} \in BZ} [\tau_{CP}^{-1} - B(E, \mathbf{k})]_{k'\sigma'L',k\sigma L}^{-1}$$

## CPA condition

$$G^{CP} = c_A G_A + c_B G_B + c_C G_C + \dots + c_N G_N$$

CPA crystal consists of ‘disordered’ nodes arranged with translation symmetry of cell and mimics alloys, defects, etc.

KKR-CPA code allows for treat many atoms on disordered sites ( $N > 10$ ) solved self-consistently.  
*Muffin-tin* potential is used due to CPA condition, defined for spherical potentials.

# KKR-CPA method for disordered alloys

## Korringa-Kohn-Rostoker with coherent potential approximation

$$G(E) = \sum_{s=(+,-)} \sum_{k=1}^K \int_{V_k} d^3r \langle s, \mathbf{r} + \mathbf{a}_k | G(E) | s, \mathbf{r} + \mathbf{a}_k \rangle.$$

*Bansil, Kaprzyk, Mijnaerends, JT, Phys. Rev. B (1999)* **conventional KKR**

**Full GF**

*Stopa, Kaprzyk, JT, J.Phys.CM (2004)* **novel formulation of KKR**

$$\langle s', \mathbf{r}' + \mathbf{a}_{k_{CP}} | G^{A(B)}(E) | s, \mathbf{r} + \mathbf{a}_{k_{CP}} \rangle$$

$$= - \sum_{\sigma L} J_{\sigma L}^{A(B)}(s' \mathbf{r}') Z_{\sigma L}^{A(B)}(s \mathbf{r})$$

$$+ \sum_{\sigma' L', \sigma L} Z_{\sigma' L'}^{A(B)}(s' \mathbf{r}') T_{k_{CP} \sigma' L', k_{CP} \sigma L}^{A(B)} Z_{\sigma L}^{A(B)}(s \mathbf{r})$$

$$G(E) = - \frac{d}{dE} \left\{ \frac{1}{N} \sum_{\mathbf{k} \in BZ} \text{Tr} \ln [G_0^{-1}(E, \mathbf{k}) + D^{(j)} - D_{CP}]^{-1} \right\}$$

$$- \frac{d}{dE} \{ c_A \text{Tr} \ln [\Psi_A^{-1} G^A] + c_B \text{Tr} \ln [\Psi_B^{-1} G^B] - \text{Tr} \ln G^{CP} \} + \frac{d}{dE} \left\{ \sum_{k \neq k_{CP}} \text{Tr} \ln [\Psi^{(k)}] \right\}, \quad (2.22)$$

$$\langle s', \mathbf{r}' + \mathbf{a}_{k'} | G(E) | s, \mathbf{r} + \mathbf{a}_k \rangle$$

$$= - \sum_{\sigma L} J_{\sigma L}^{(k)}(s' \mathbf{r}') Z_{\sigma L}^{(k)}(s \mathbf{r}) \delta_{kk'}$$

$$+ \sum_{\sigma' L', \sigma L} Z_{\sigma' L'}^{(k')} (s' \mathbf{r}') T_{k' \sigma' L', k \sigma L}^{CP} Z_{\sigma L}^{(k)}(s \mathbf{r})$$

$$T_{k' \sigma' L', k \sigma L}^{CP} = \frac{1}{N} \sum_{\mathbf{k} \in BZ} [\tau_{CP}^{-1} - B(E, \mathbf{k})]_{k' \sigma' L', k \sigma L}^{-1}$$

CPA  $c_A T^A + c_B T^B = T^{CP}$ .

Density of states  $N(E) = - \frac{1}{\pi} \text{Im} \int_{-\infty}^E dE G(E)$

Lloyd formula *Kaprzyk et al. Phys. Rev. B (1990)*

Fermi energy  $N(E_F) = Z$

# Electron transport coefficients

$$\sigma_e = \mathcal{L}^{(0)},$$

**Electrical conductivity**

$$S = -\frac{1}{eT} \frac{\mathcal{L}^{(1)}}{\mathcal{L}^{(0)}},$$

**Seebeck coefficient (thermopower)**

$$\kappa_e = \frac{\mathcal{L}^{(2)}}{e^2 T} - \frac{\mathcal{L}^{(1)} \mathcal{L}^{(1)}}{e^2 T \mathcal{L}^{(0)}}$$

**Electronic thermal conductivity**

$$L(T) = \frac{\kappa_e(T)}{\sigma(T)T} \quad \text{Wiedemann-Franz-Lorenz}$$

$$L = \frac{\kappa_e}{\sigma T}$$

$$PF = S^2 \sigma$$

## Onsager-related functions

$$\mathcal{L}^{(\alpha)} = \int d\mathcal{E} \left( -\frac{\partial f}{\partial \mathcal{E}} \right) (\mathcal{E} - \mu)^\alpha \sigma(\mathcal{E})$$

$$ZT = \frac{S^2 \sigma T}{\kappa_e + \kappa_l}$$

$$L(T, n)$$

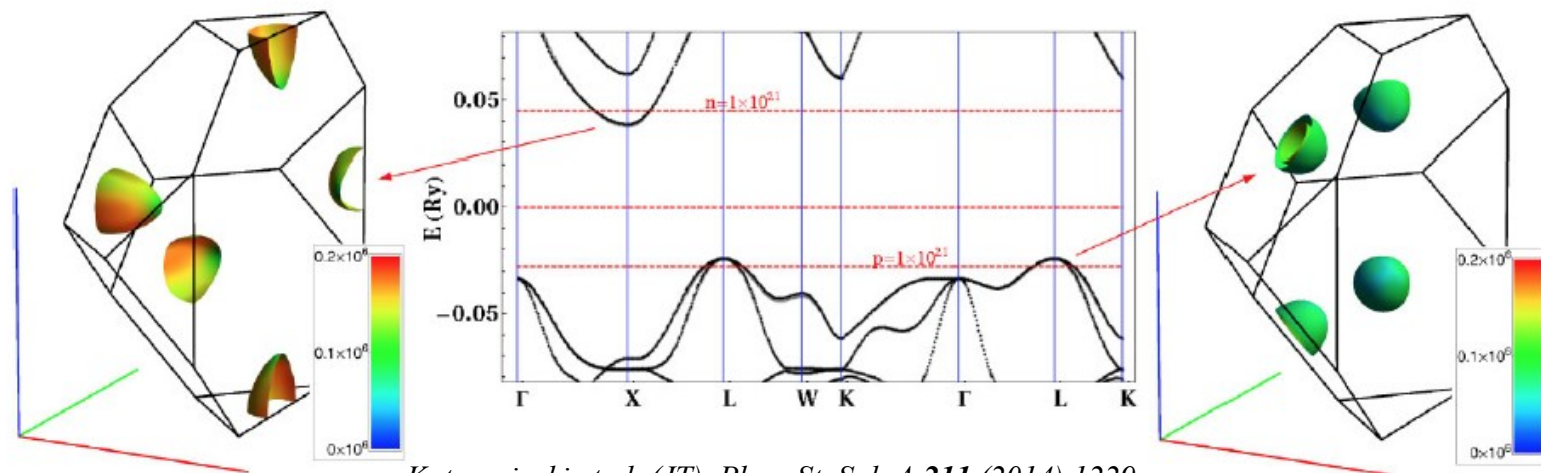
$$PF(T, n)$$

$$ZT(T, n)$$

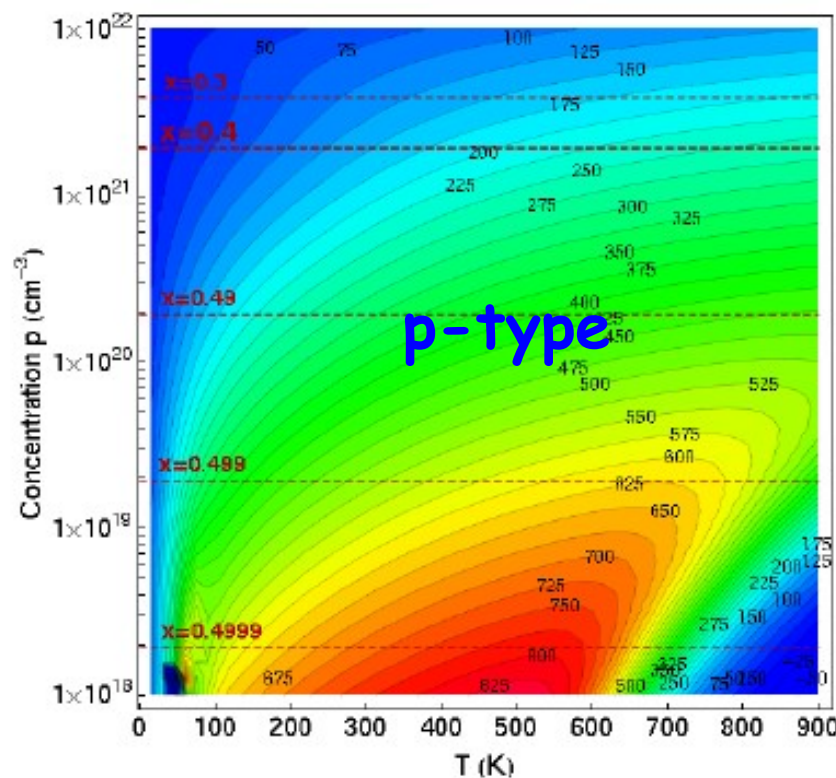
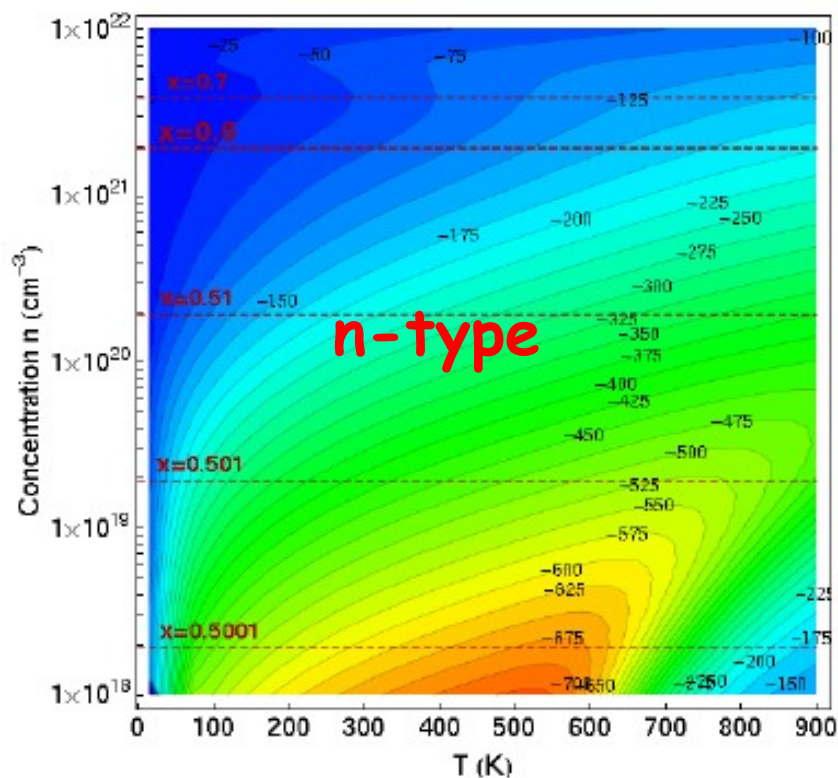
## Transport functions (in general tensors)

$$\sigma(\mathcal{E}) = e^2 \sum_n \int \frac{d\mathbf{k}}{4\pi^3} \tau_n(\mathbf{k}) \mathbf{v}_n(\mathbf{k}) \otimes \mathbf{v}_n(\mathbf{k}) \delta(\mathcal{E} - \mathcal{E}_n(\mathbf{k}))$$

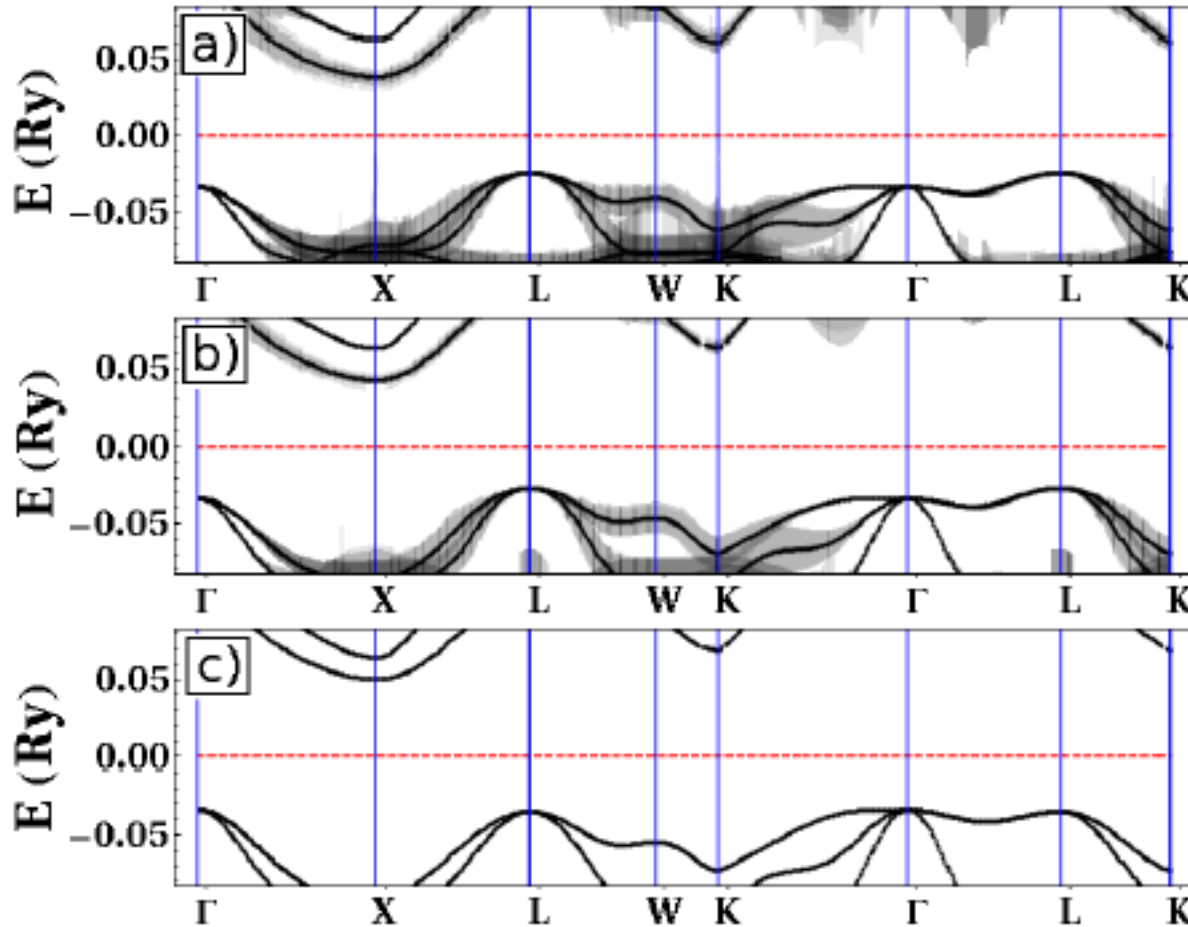
# Seebeck coefficient vs. temperature & carrier concentration



*Kutorasinski et al. (JT), Phys. St. Sol. A 211 (2014) 1229*

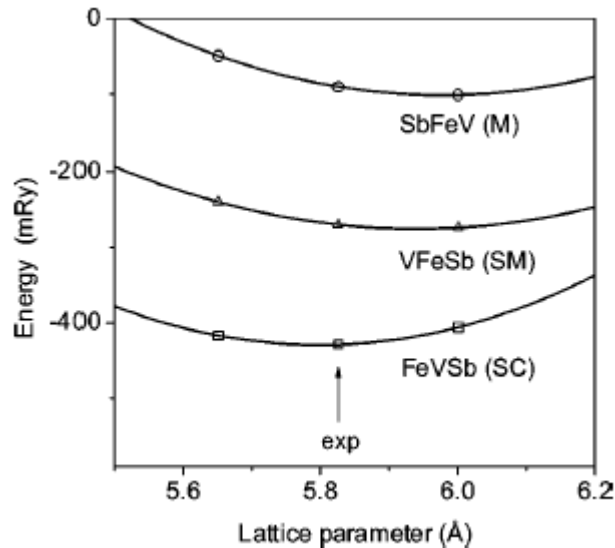
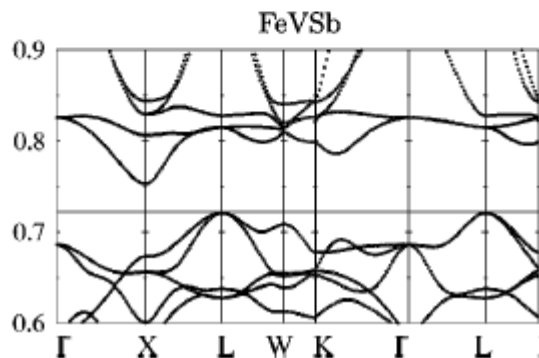
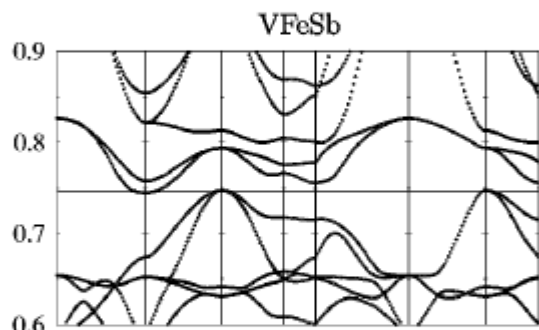
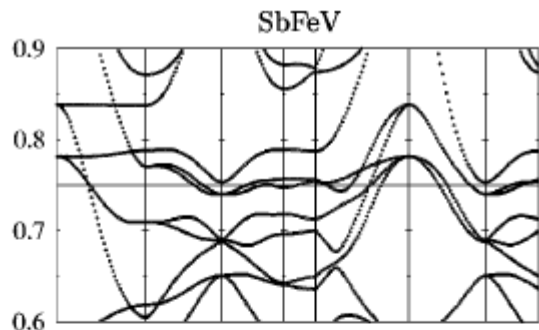
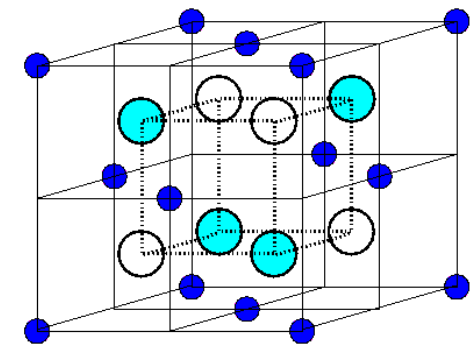


# Complex energy band „engineering”



Tendency to **alignment of bands** near Fermi energy  
BUT it needs experimental proof whether TE properties are really improved

# Role of point defects FeVSb – “dirty” semiconductor

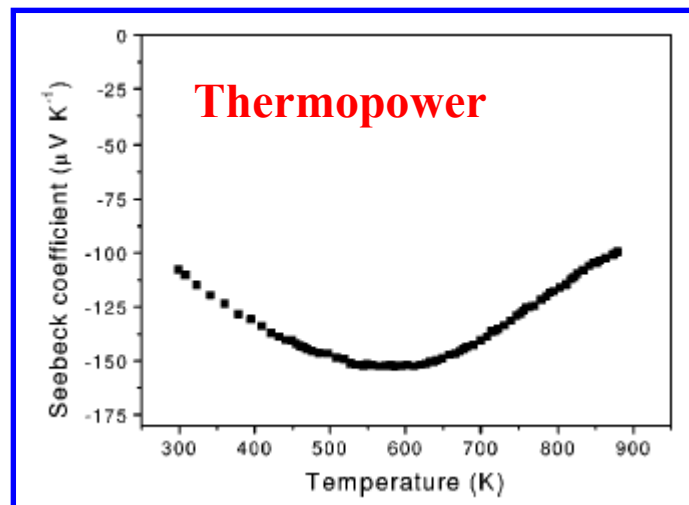
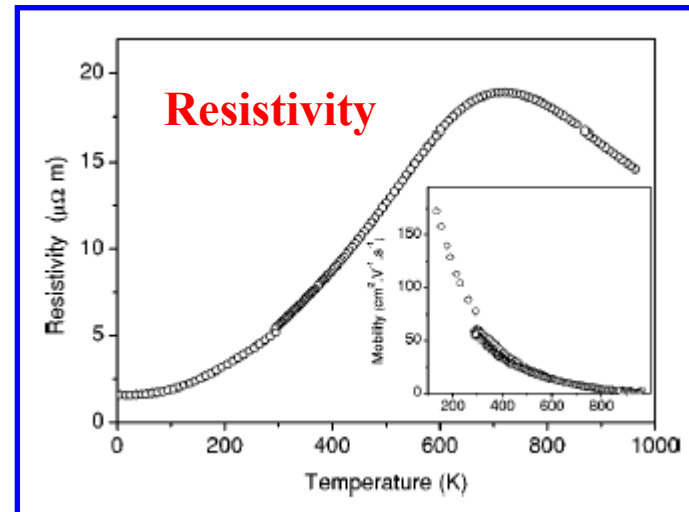


KKR-CPA – total energy

Defects should be accounted :  
to interpret metallic electron  
conductivity + large Seebeck  
coefficient

FeVSb - rather semiconductor

Jodin, JT, ..., PRB (2004)



# Defects in Heusler alloys

Nominal	EMPA
FeVSb	$\text{Fe}_{0.98}\text{V}_{0.99}\text{Sb}_{1.03}$
$\text{Fe}_{0.995}\text{Co}_{0.005}\text{VSb}$	$\text{Fe}_{0.97}\text{Co}_{0.006}\text{V}_{0.99}\text{Sb}_{1.03}$
$\text{Fe}_{0.98}\text{Co}_{0.02}\text{VSb}$	$\text{Fe}_{0.95}\text{Co}_{0.02}\text{V}_{1.02}\text{Sb}_{1.01}$
$\text{FeV}_{0.90}\text{Ti}_{0.10}\text{Sb}$	$\text{Fe}_{0.96}\text{V}_{0.9}\text{Ti}_{0.1}\text{Sb}_{1.04}$
$\text{FeV}_{0.85}\text{Ti}_{0.15}\text{Sb}$	$\text{Fe}_{0.98}\text{V}_{0.86}\text{Ti}_{0.15}\text{Sb}_{1.01}$
$\text{FeV}_{0.80}\text{Ti}_{0.20}\text{Sb}$	$\text{Fe}_{0.99}\text{V}_{0.77}\text{Ti}_{0.22}\text{Sb}_{1.02}$
$\text{FeV}_{0.95}\text{Zr}_{0.05}\text{Sb}$	$\text{Fe}_{0.95}\text{V}_{0.98}\text{Zr}_{0.02}\text{Sb}_{1.05}$
$\text{FeV}_{0.90}\text{Zr}_{0.10}\text{Sb}$	$\text{Fe}_{0.96}\text{V}_{0.97}\text{Zr}_{0.03}\text{Sb}_{1.04}$
$\text{FeV}_{0.85}\text{Zr}_{0.15}\text{Sb}$	$\text{Fe}_{0.95}\text{V}_{0.93}\text{Zr}_{0.07}\text{Sb}_{1.05}$

EPMA data

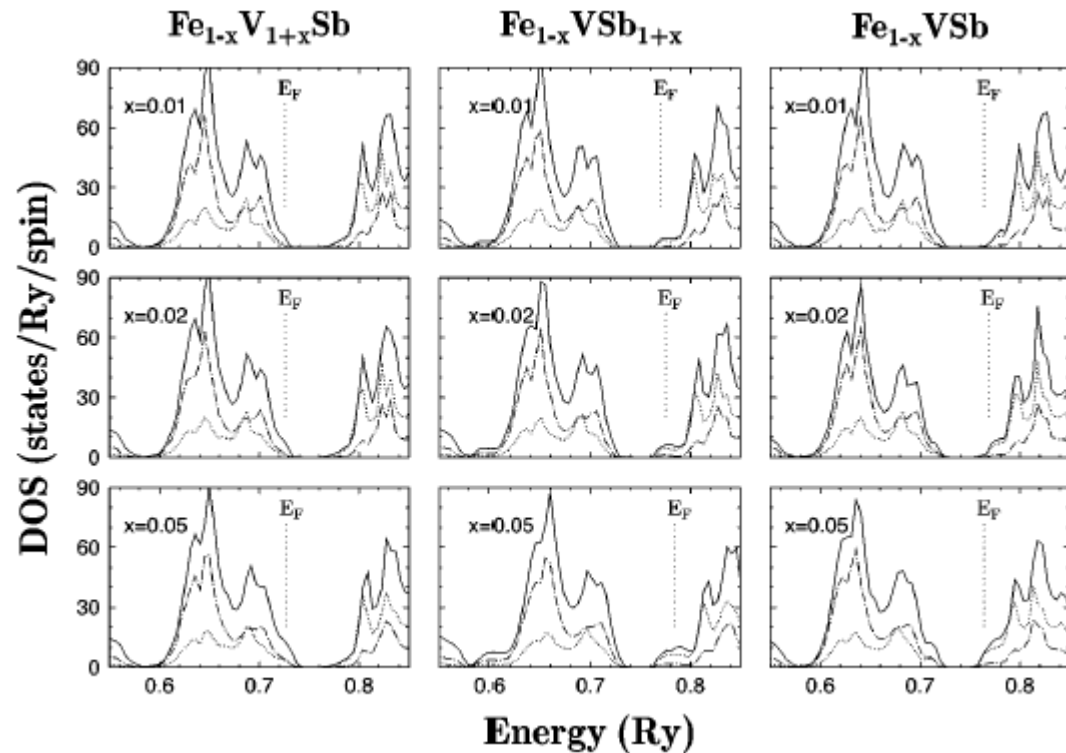
## Doping of n and p types

TABLE IV. Room temperature Seebeck coefficient  $S$  and resistivity  $\rho$  in pure and substituted FeVSb half-Heusler phases.

Composition	$\rho$ ( $\mu\Omega$ m)	$S$ ( $\mu\text{V K}^{-1}$ )	$n \times 10^{20}(\text{cm}^{-3})$
FeVSb	5.1	-110	$\approx 1$
$\text{Fe}_{0.995}\text{Co}_{0.005}\text{VSb}$	4.2	-130	$\approx 1$
$\text{Fe}_{0.98}\text{Co}_{0.02}\text{VSb}$	2.3	-80	$\approx 5$
$\text{FeV}_{0.95}\text{Ti}_{0.05}\text{Sb}$	13	+180	$\approx 5$
$\text{FeV}_{0.90}\text{Ti}_{0.10}\text{Sb}$	15.5	+145	$\approx 5$
$\text{FeV}_{0.85}\text{Ti}_{0.15}\text{Sb}$	68.7	+125	$\approx 2$
$\text{FeV}_{0.80}\text{Ti}_{0.20}\text{Sb}$	20	+70	$\approx 20$
$\text{FeV}_{0.95}\text{Zr}_{0.02}\text{Sb}$	46	-20	$\approx 1$
$\text{FeV}_{0.90}\text{Zr}_{0.03}\text{Sb}$	43	+20	$\approx 3$
$\text{FeV}_{0.85}\text{Zr}_{0.07}\text{Sb}$	23	+30	$\approx 4$

KKR-CPA density of states upon inclusion Fe/Sb vac/Fe defects

Vacancy on Fe-site & Sb on Fe-site behaves as a HOLE donor

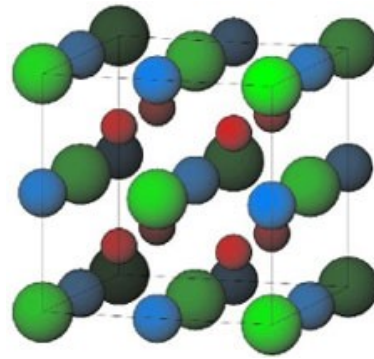


Jodin, JT, ..., PRB (2004)



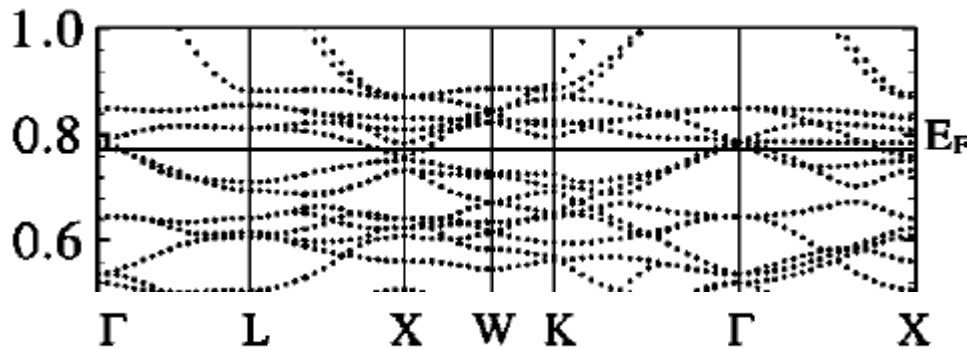
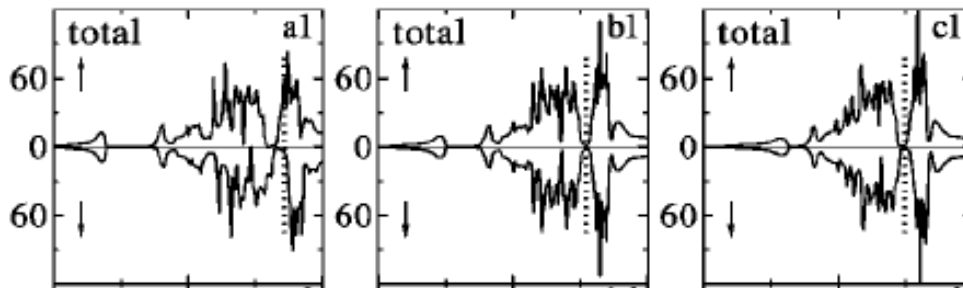
# Fe<sub>2</sub>VAl i Fe<sub>2</sub>VGa semimetals

theory

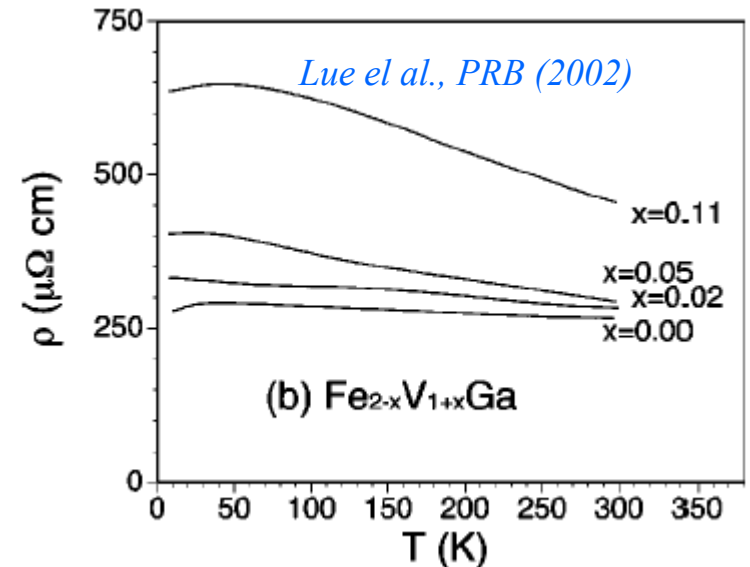
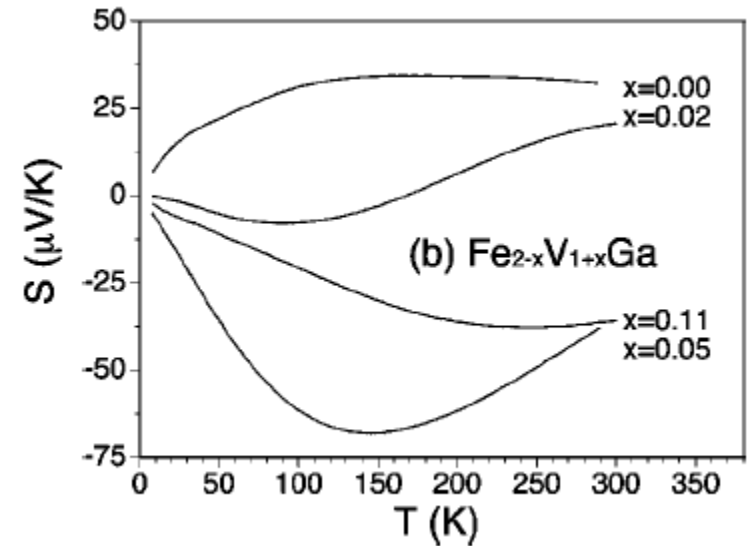


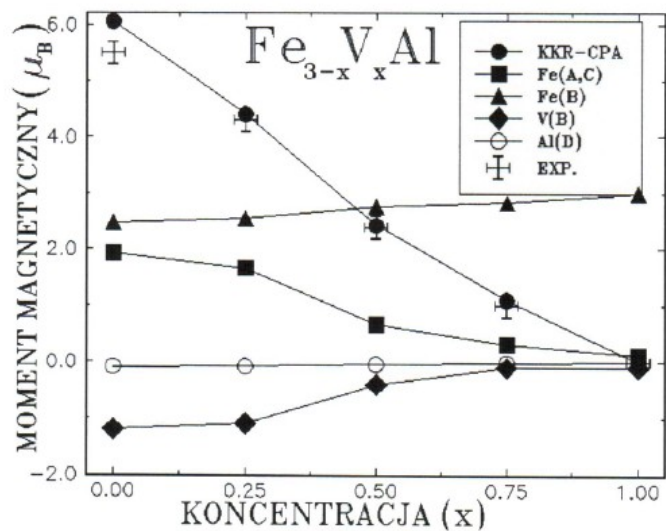
*Bansil, ... JT, PRB 60(1999) 13397*

Fe<sub>2</sub>VSi      Fe<sub>2</sub>VGa      Fe<sub>2</sub>VAl



experiments



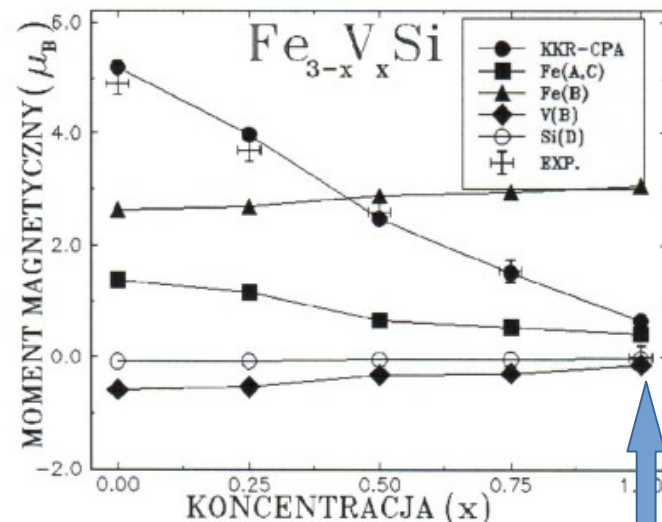


**Fe<sub>2</sub>VSi**  
weak ferromagnet

VEC=25

**Fe<sub>2</sub>VAl**  
pseudogap

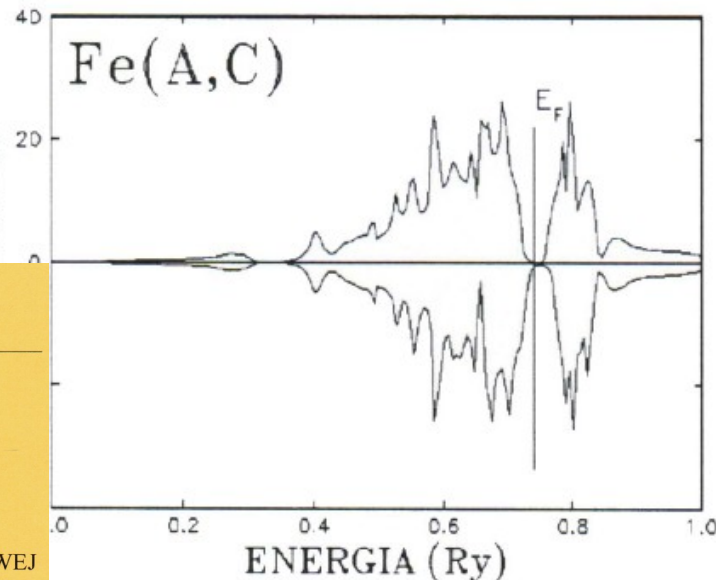
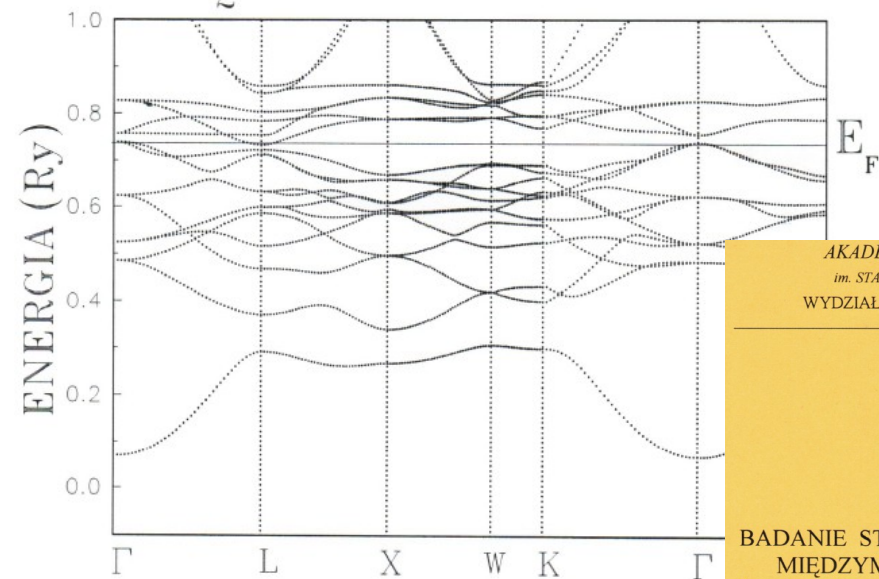
VEC=24



0.37μ<sub>B</sub> (exp)

0.42μ<sub>B</sub> (theory)

Fe<sub>2</sub>VAl



AKADEMIA GÓRNICZO-HUTNICZA  
im. STANISŁAWA STASZICA w KRAKOWIE  
WYDZIAŁ FIZYKI I TECHNIKI JĄDROWEJ

---

Praca doktorska

**1994**

Janusz Tobała

---

BADANIE STRUKTURY ELEKTRONOWEJ  
MIĘDZYMETALICZNYCH STOPÓW  
ŻELAZA METODAMI TEORII PASMOWEJ

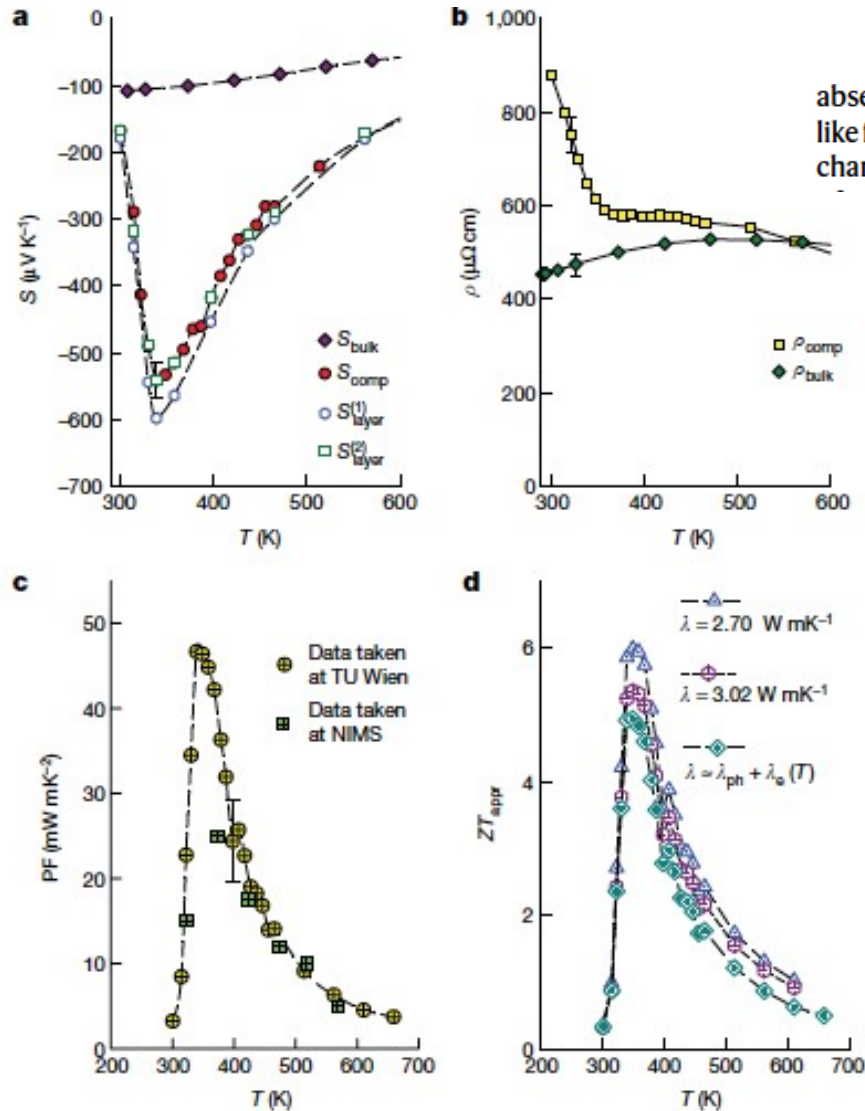
Article

# Thermoelectric performance of a metastable thin-film Heusler alloy

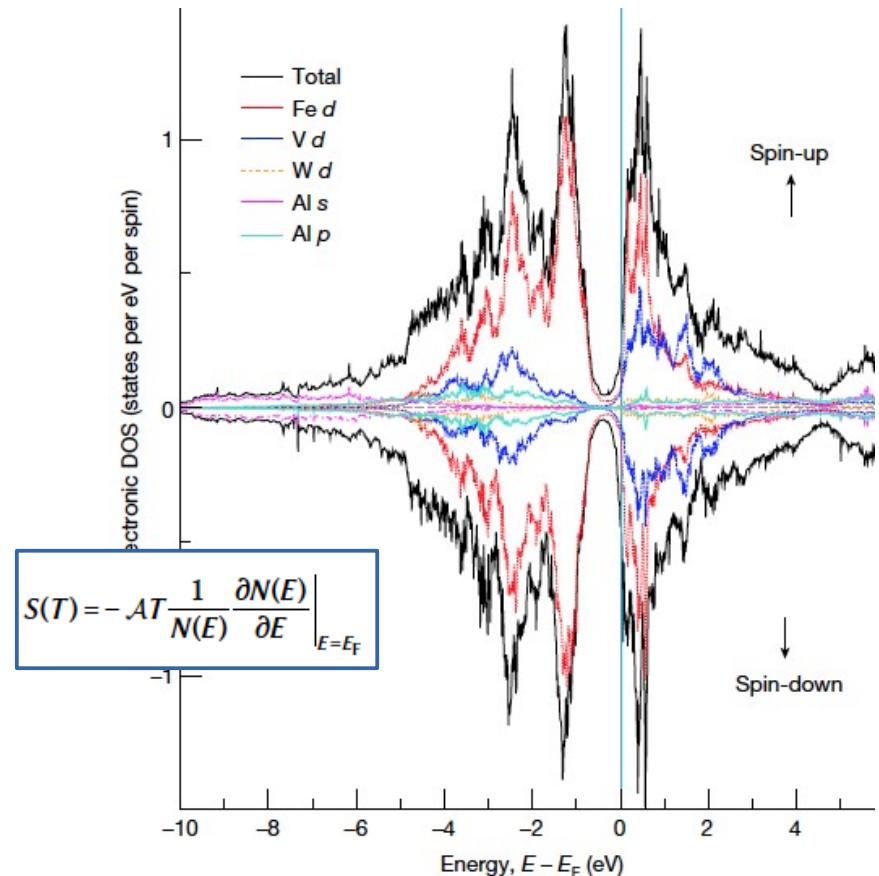
## Fe<sub>2</sub>(V-W)Al

ZT ~ 6 !!!

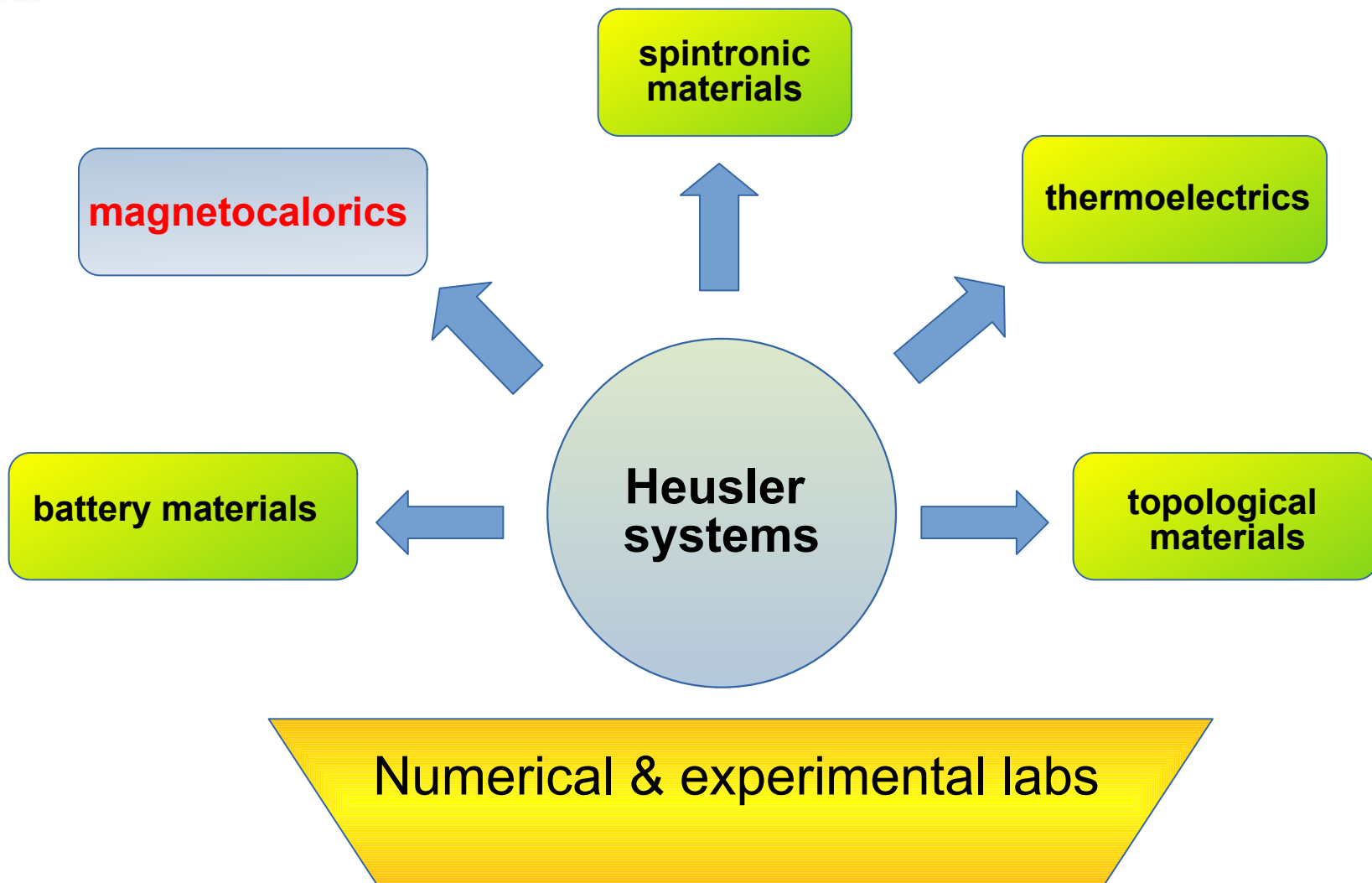
the largest ZT ever measured



absent. In other words, bcc-type Fe<sub>2</sub>V<sub>0.8</sub>W<sub>0.2</sub>Al exhibits potential Weyl-like fermions around the Fermi level for both the spin-up and spin-down channels, thereby leading to a possible profound, non-trivial topology



$$S(T) = -AT \left. \frac{1}{N(E)} \frac{\partial N(E)}{\partial E} \right|_{E=E_F}$$



# Brief history of MCE discovery

**1881** E. Warburg, iron heats up in magnetic field  $\sim 0.5\text{-}2\text{ K/1T}$ , Ann. Phys. (1881)

**1926** P. Debye (Nobel 1936, chemistry)

**1927** W. Giauque (Nobel 1949, chemistry)

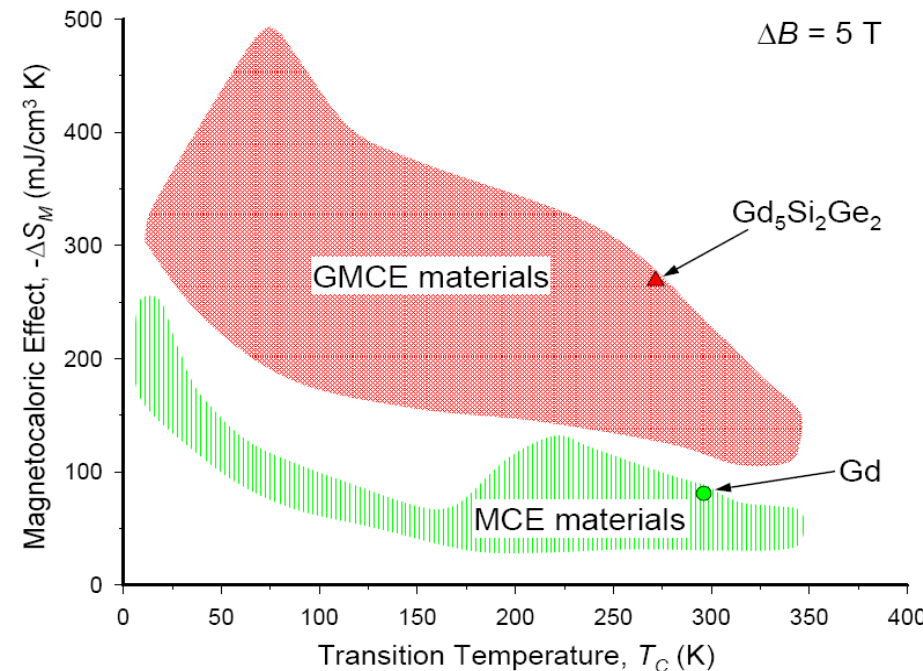
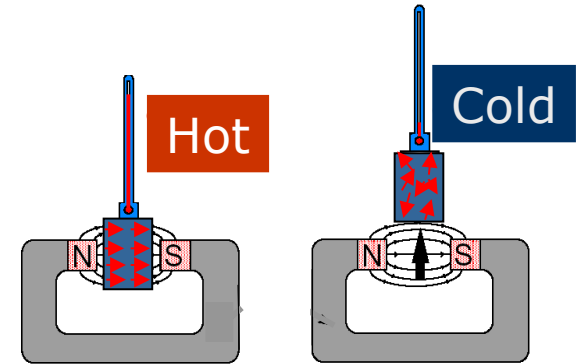
cooling via adiabatic demagnetization (order-disorder transition of magnetic moments in presence (or not) of magnetic field; for cryogenic purposes, down to 0.25 K (MacDougall, 1933).

**1997** K. A. Gschneider & V. Pecharsky (Ames Lab., USA), PRL (1997) - discovery of giant magnetocaloric effect :

MCE: an intrinsic property of magnetic materials;

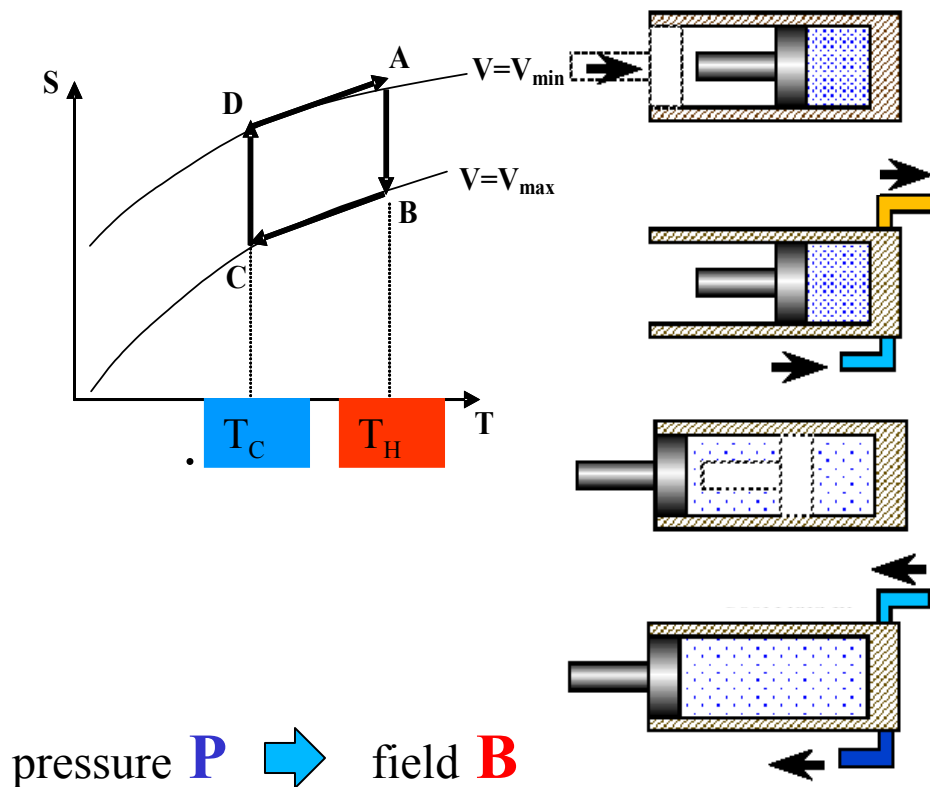
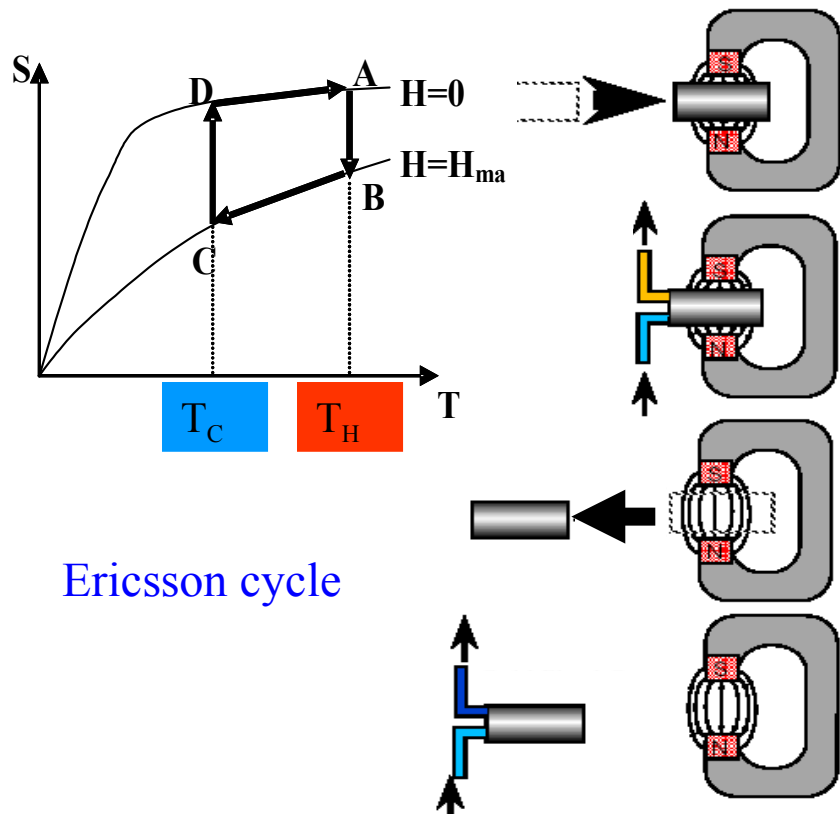
MCE : the largest at the transition temperature, e.g. ferro-para

Adiabatic magnetization / demagnetisation



# Analogy to thermodynamic cycle

## Adiabatic magnetization/demagnetization



$$B \cdot (M_1 - M_2) = \Delta S \cdot \Delta T = -RCP$$

Ideal Carnot cycle :

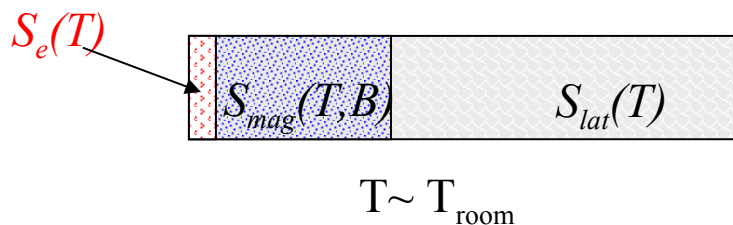
$$\eta = \frac{\Delta W}{\Delta Q_H} = 1 - \frac{T_C}{T_H}$$

$$\Delta W = \oint P dV = (T_H - T_C)(S_B - S_A)$$

$$\Delta Q_C = T_C(S_B - S_A)$$

$$\Delta Q_H = T_H(S_B - S_A)$$

# Entropy



$$S_{tot} = S_{el} + S_{mag} + S_{lat}$$

$$\Delta S_{mag} \uparrow + \Delta S_{lat} \downarrow = 0$$

**Adiabatic Process**

$$\Delta S_{mag}(T, \Delta B) = \int_0^B \left( \frac{\partial M}{\partial T} \right)_B dB$$

$$\Delta S_{lat} = C_p(B, T) \frac{\Delta T}{T}$$

$$\Delta T_{max} = \frac{-T \Delta S_{mag}}{C_p(B, T)}$$

Calorific Capacity

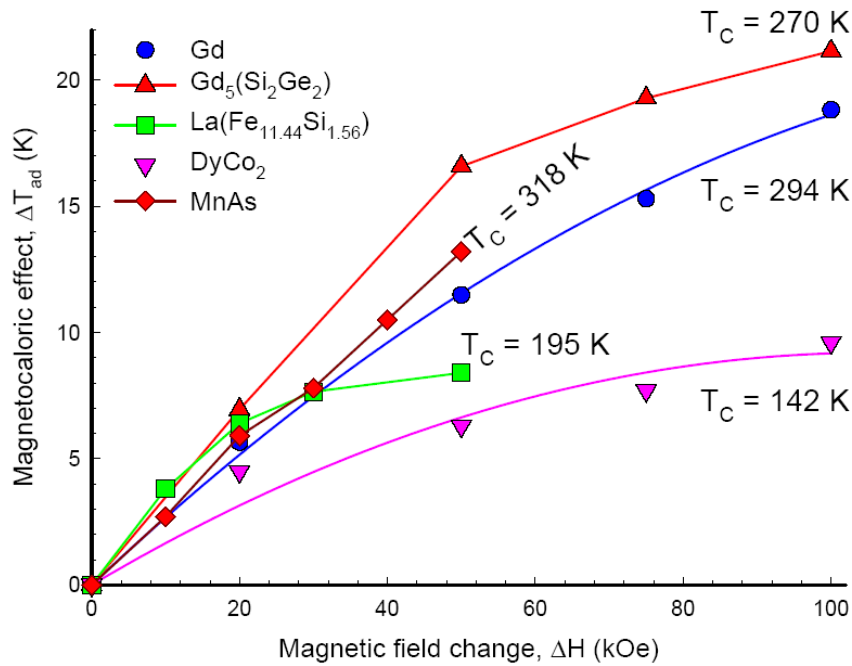
$$C_p(B, T)$$

Magnetic Entropy

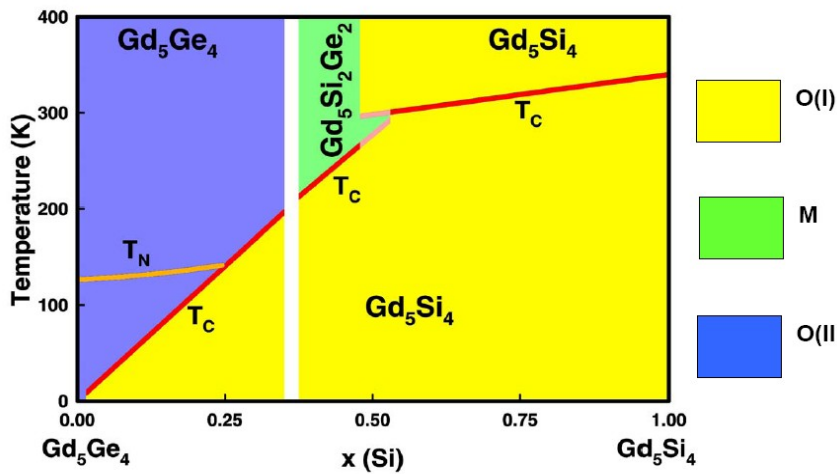
$$\Delta S_{mag}$$

$$\Delta T_{max}$$

# New MCE materials

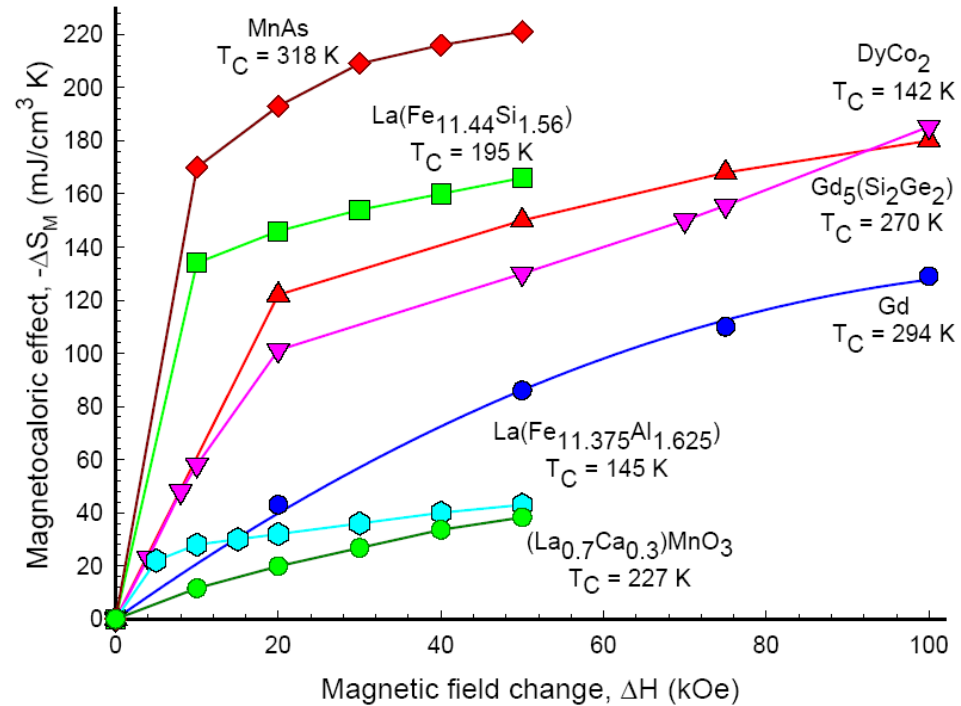


## Temperature jump



Seminarium WFIS, 21.05.2021, Kraków

From K Gschneider

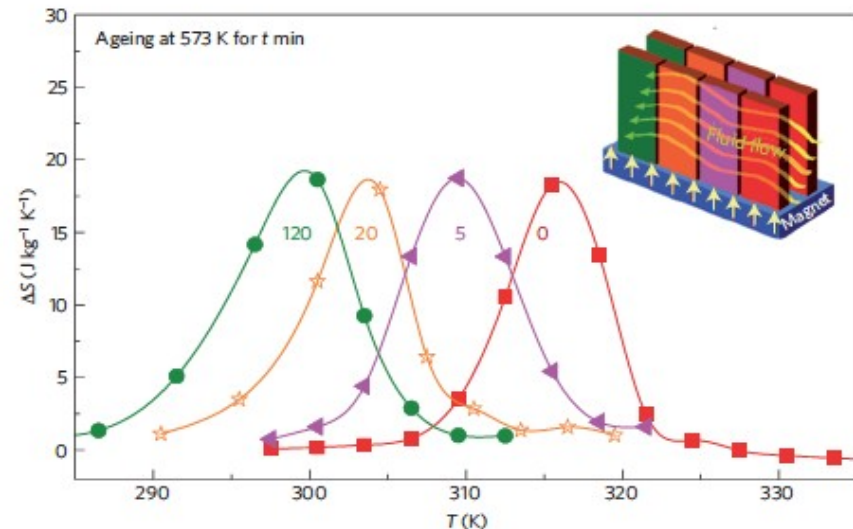
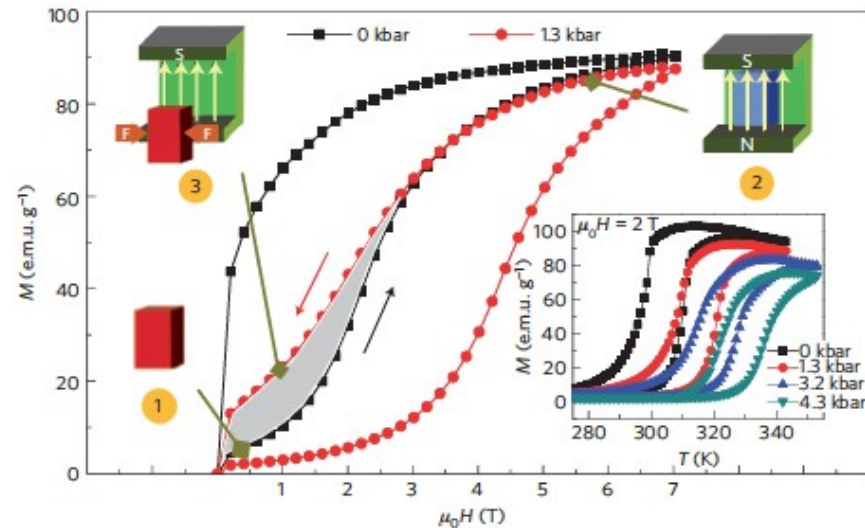
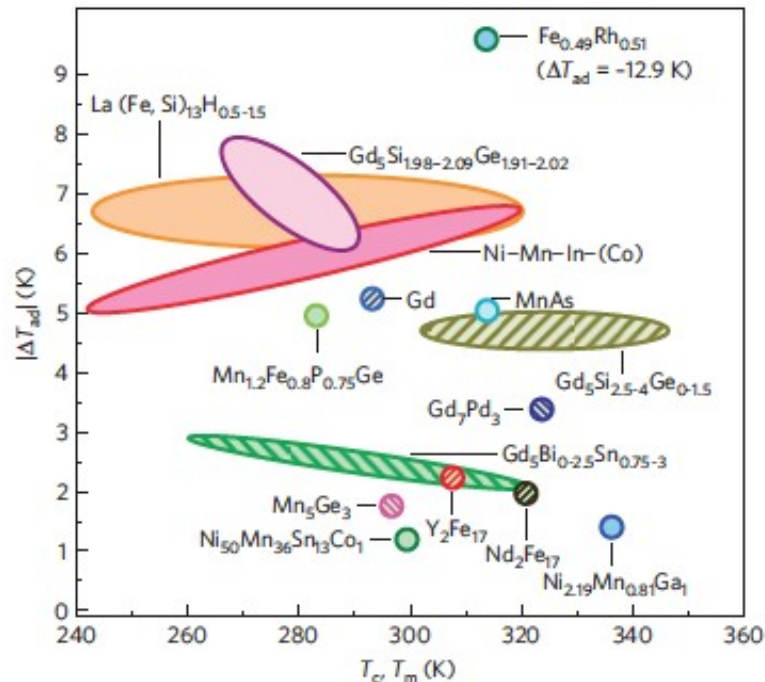


## Entropy jump



# Heusler systems as magnetocaloric materials

## Ni<sub>2</sub>MnIn + Co magnetic shape memory alloys



ARTICLES

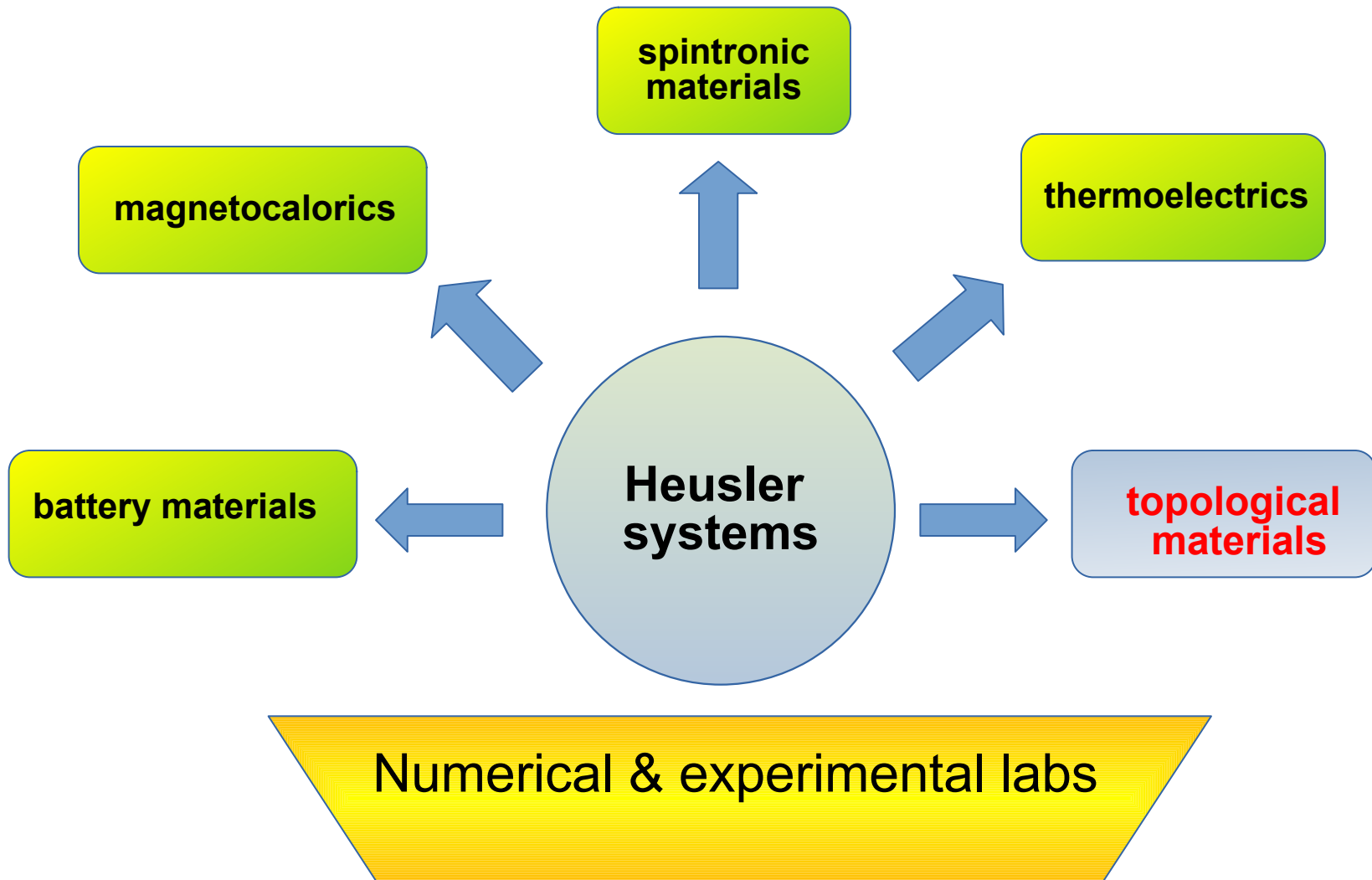
PUBLISHED ONLINE: 27 MAY 2012 | DOI: 10.1038/NMAT3334

nature  
materials

## Giant magnetocaloric effect driven by structural transitions

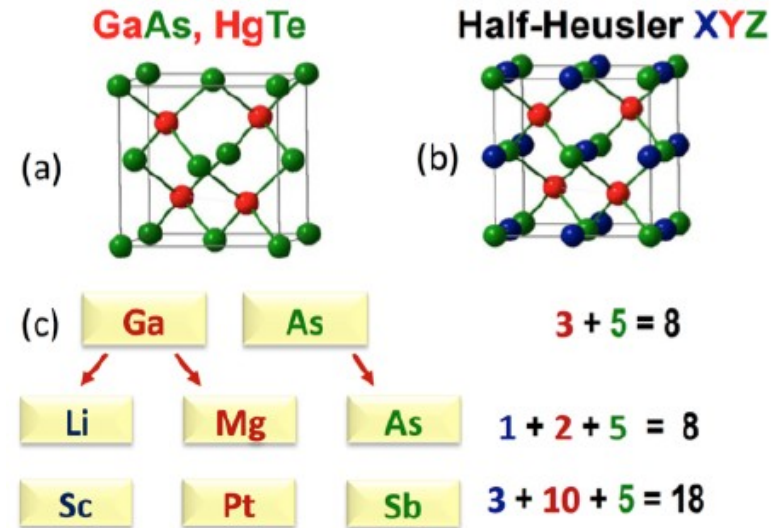
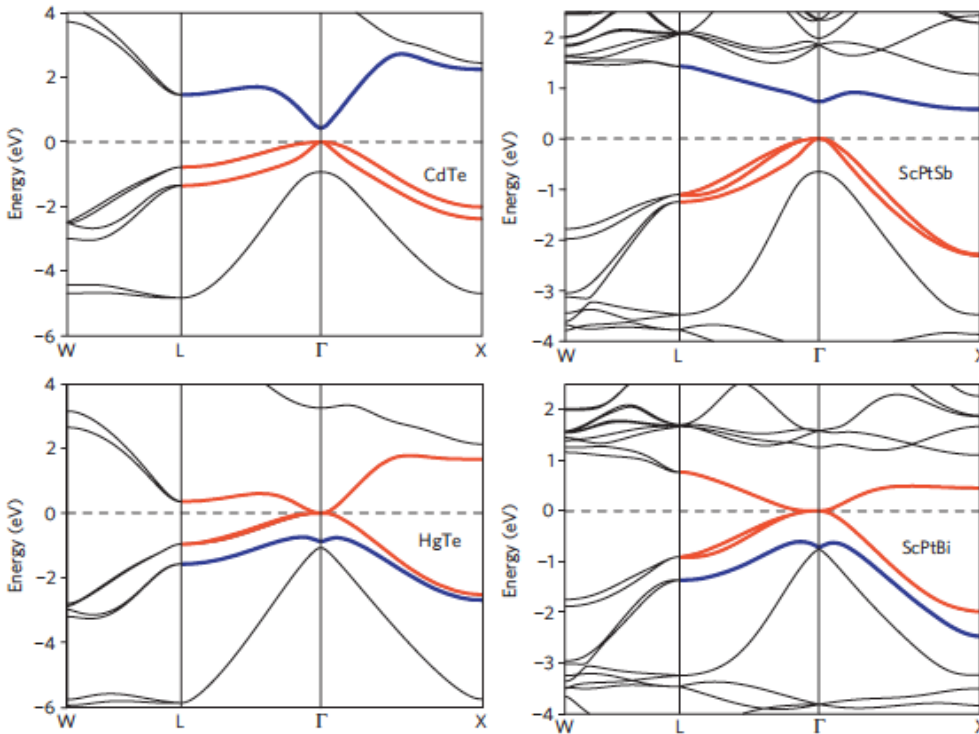
Jian Liu<sup>1\*</sup>, Tino Gottschall<sup>1\*</sup>, Konstantin P. Skokov<sup>1</sup>, James D. Moore<sup>1</sup> and Oliver Gutfleisch<sup>1,2</sup>

Seminarium WFIS, 21.05.2021, Kraków



## Tunable multifunctional topological insulators in ternary Heusler compounds

Stanislav Chadov<sup>1</sup>, Xiaoliang Qi<sup>2,3</sup>, Jürgen Kübler<sup>4</sup>, Gerhard H. Fecher<sup>1</sup>, Claudia Felser<sup>1\*</sup> and Shou Cheng Zhang<sup>3\*</sup>

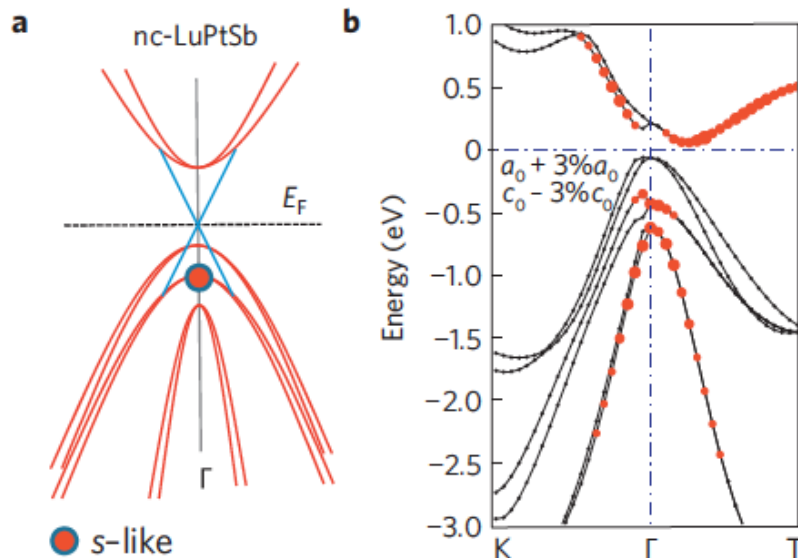


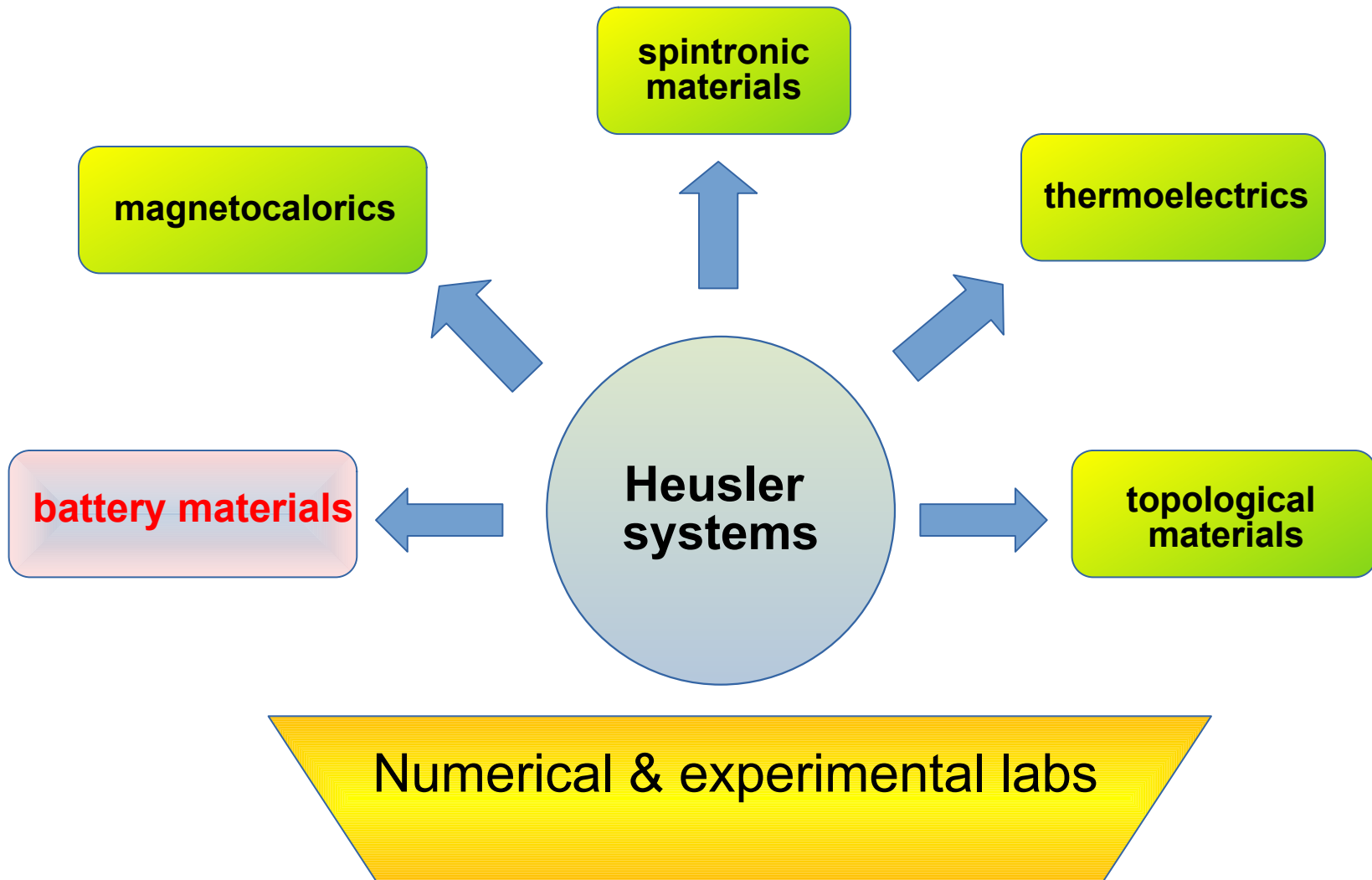
from: B. Yan & A. de Visse

## Half-Heusler ternary compounds as new multifunctional experimental platforms for topological quantum phenomena

Hsin Lin<sup>1</sup>, L. Andrew Wray<sup>2</sup>, Yuqi Xia<sup>2</sup>, Suyang Xu<sup>2</sup>, Shuang Jia<sup>3</sup>, Robert J. Cava<sup>3</sup>, Arun Bansil<sup>1</sup> and M. Zahid Hasan<sup>2,4,5\*</sup>

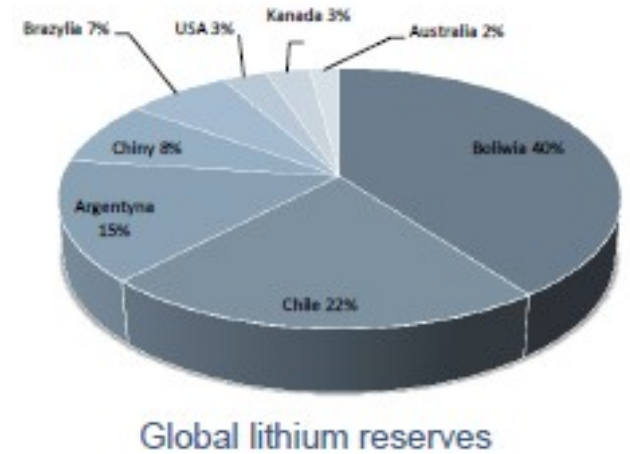
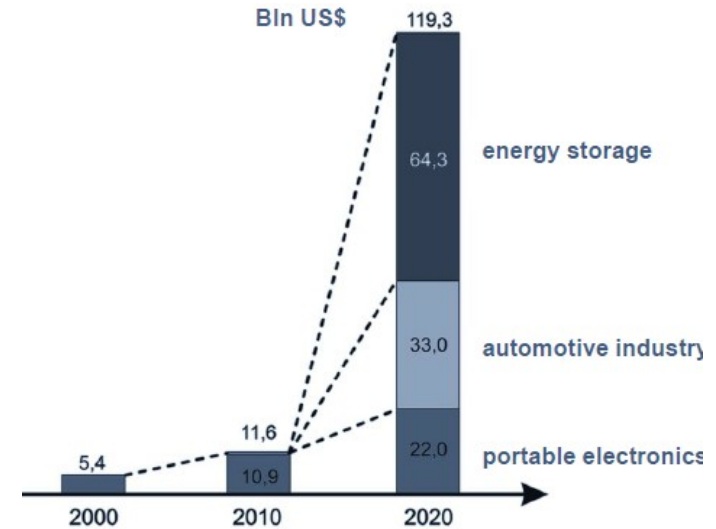
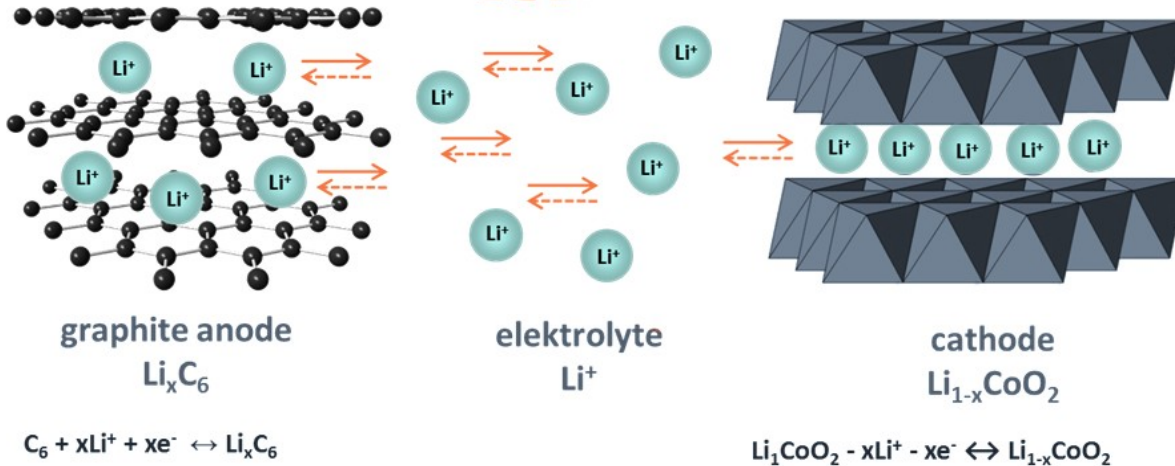
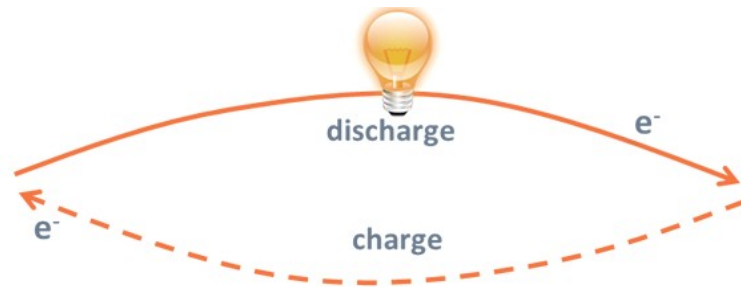
Seminarium WFIS, 21.05.2021, Kraków





# Li-ion battery cathode materials

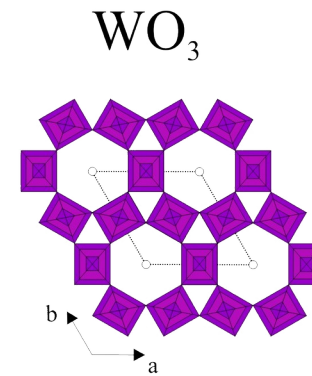
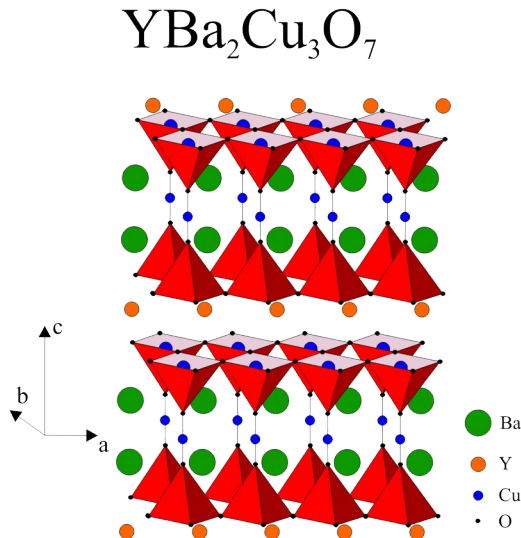
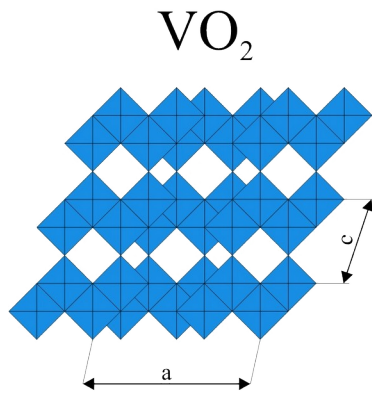
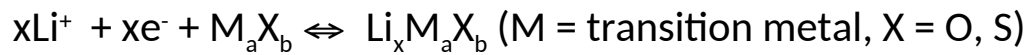
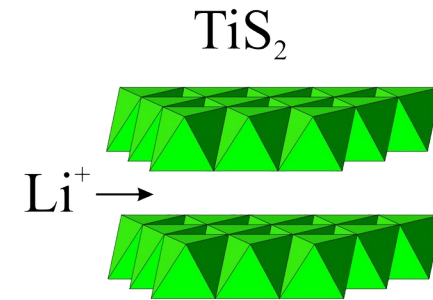
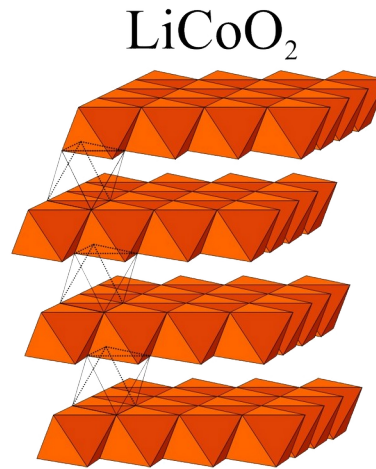
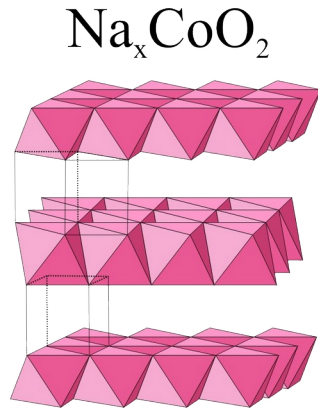
Must be gradually replaced by Na-ion battery?  
*world's resources of Li likely insufficient...*



Kim et al. Adv. Energy Mater. 2 (2012) 860.

from J. Molenda

# Types of crystal structure capable for alkaline-ion intercalation





# Heusler alloys as battery materials?

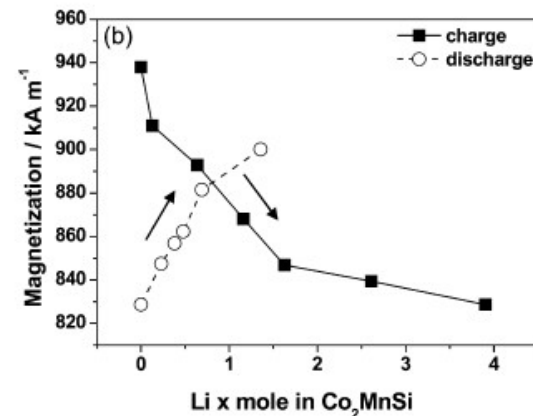
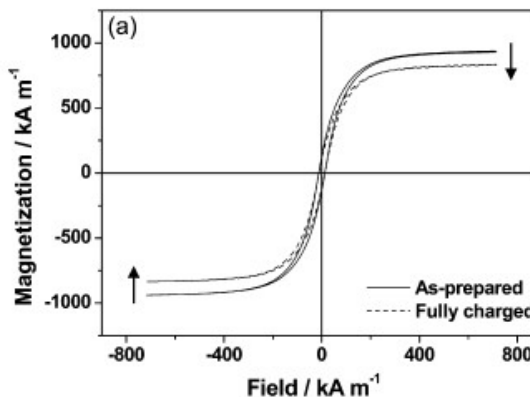
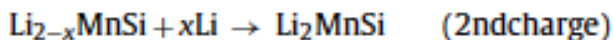
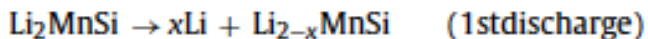
Short communication

## Electrochemical behaviour of Heusler alloy $\text{Co}_2\text{MnSi}$ for secondary lithium batteries

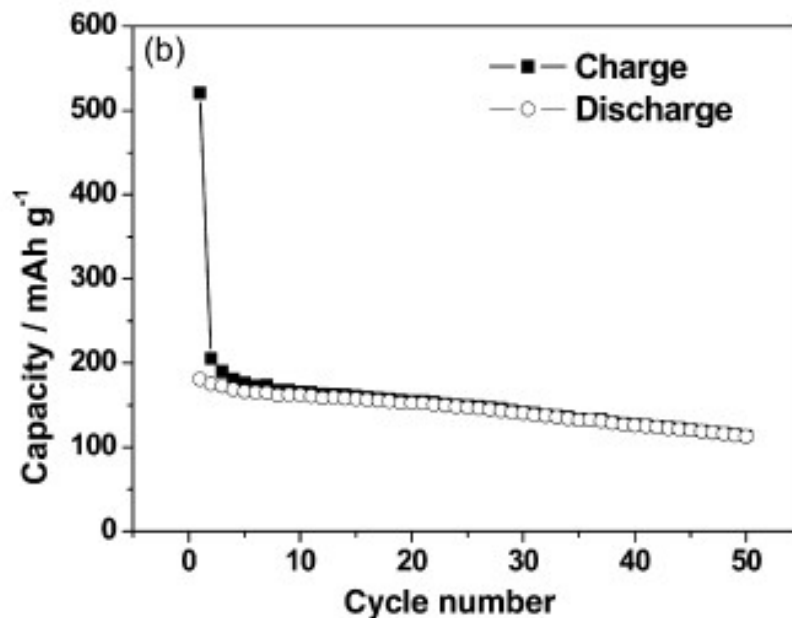
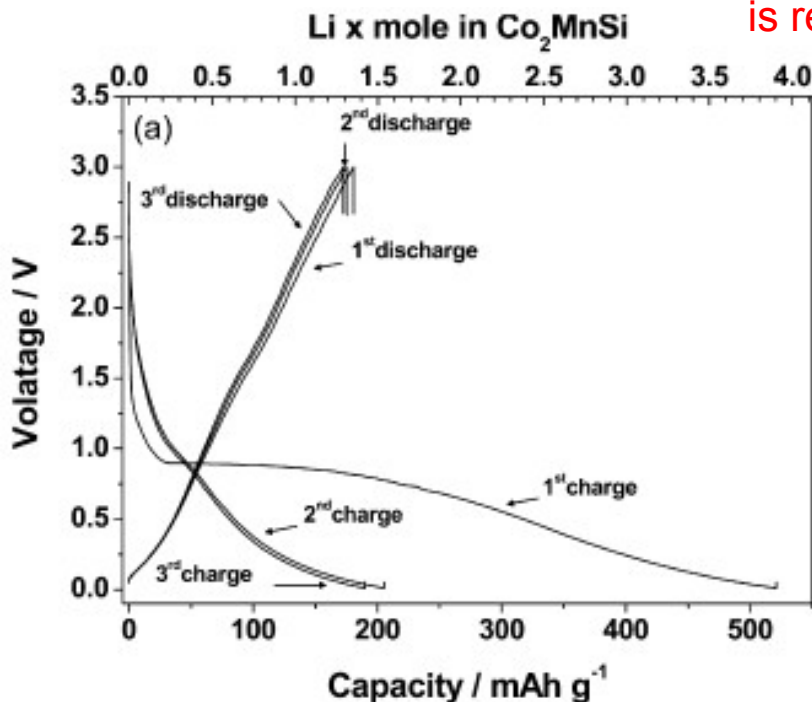
Jun H. Park<sup>a</sup>, Dae H. Jeong<sup>a</sup>, Sang M. Cha<sup>a</sup>, Yang-Kook Sun<sup>b</sup>, Chong S. Yoon

<sup>a</sup> Department of Materials Science and Engineering, Hanyang University, Seoul 133-791, Republic of Korea

<sup>b</sup> Department of Chemical Engineering, Hanyang University, Seoul 133-791, Republic of Korea



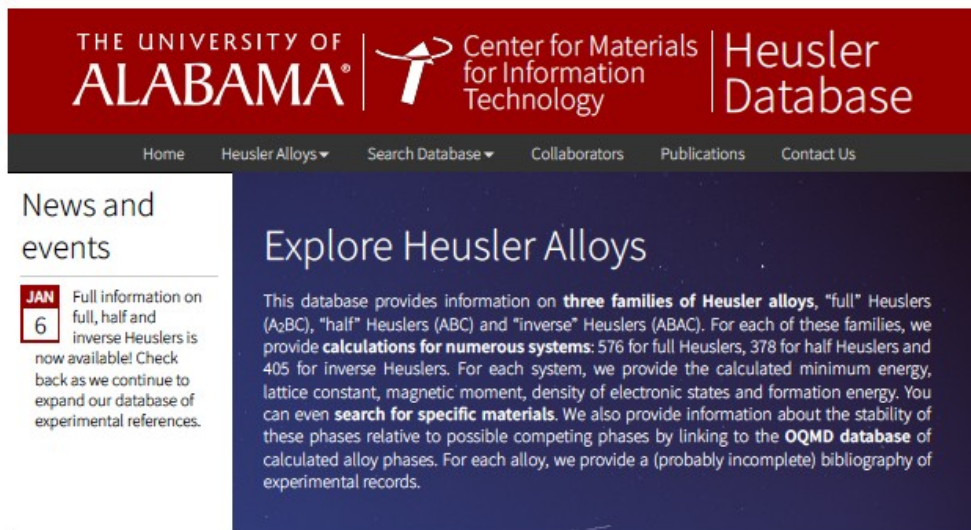
Li may substitute Co or Mn, depending on relative chemical potentials  
BUT magnetisation measurements confirm that Co is replaced



# Summary

Heusler alloys exhibit outstanding variety of physical properties, which are related to particular **interplay of electronic structure features and crystal structure**.

The fact that 3, 4 (or more) different atoms occupy 4 equivalent *fcc* sublattices seems to be responsible for **exceptional richness of observed physical behaviors**, but also result in a presence of different forms of disorder (chemical, topological).



THE UNIVERSITY OF ALABAMA | Center for Materials for Information Technology | Heusler Database

Home Heusler Alloys Search Database Collaborators Publications Contact Us

News and events

**JAN 6** Full information on full, half and inverse Heuslers is now available! Check back as we continue to expand our database of experimental references.

### Explore Heusler Alloys

This database provides information on **three families of Heusler alloys**, "full" Heuslers ( $A_2BC$ ), "half" Heuslers ( $ABC$ ) and "inverse" Heuslers ( $ABAC$ ). For each of these families, we provide **calculations for numerous systems**: 576 for full Heuslers, 378 for half Heuslers and 405 for inverse Heuslers. For each system, we provide the calculated minimum energy, lattice constant, magnetic moment, density of electronic states and formation energy. You can even **search for specific materials**. We also provide information about the stability of these phases relative to possible competing phases by linking to the **OQMD database** of calculated alloy phases. For each alloy, we provide a (probably incomplete) bibliography of experimental records.

The properties “on request” of Heusler alloys can be easily tunable, controllable by using external fields (temperature, magnetic field, electric field, stress), doping, substitution, which already opened many opportunities for their applications.



Sponsors

The Samsung Corporation  
Supported by NSF DMREF grants no. 1235396 and 1235230  
C-SPIN is one of the six SRC STARnet Centers, sponsored by MARCO and DARPA





# Collaboration

**S. Kaprzyk, K. Kutorasiński**

*AGH University of Science and Technology, Kraków, Poland*

**B. Malaman, G. Venturini**

*Universite H. Poincare & CNRS, Nancy, France*

**L. Jodin, P. Pecheur, H. Scherrer**

*Ecole des Mines & CNRS, Nancy, France*

**J. Pierre, D. Fruchart, M. Kouacou**

*Polygone Scientifique CNRS, Grenoble, France*

**R. Skolozdra**

*I. Franko University, Lviv, Ukraine*

**K. Kaczmarska**

*Institute of Physics, Silesian University, Katowice, Poland*

Dziękuję za uwagę